

**Reply to Anonymous Referee #1 (Received and published: 11 May 2017)**

We thank the reviewer for providing us with feedback on the manuscript quickly. We have attempted to revise the manuscript based on the comments. Hope the readability of the manuscript is now improved.

This paper shows that variability in XCH<sub>4</sub> measured by satellite over India cannot be simply attributed to spatial/seasonal variability of local sources but reflects also major influences from the free troposphere. This is a simple argument and is of some interest because there is indeed temptation to make such an attribution, and the paper shows clearly that it is incorrect. The paper also presents a nice analysis of the factors controlling methane in the free troposphere over India. The scope of the paper is limited (hence my rating of "Fair") because it applies only to India, and because a more thorough analysis of XCH<sub>4</sub> data (such as with an inversion) would obviate the need for the incriminated assumption. I was hoping to get a better understanding of methane sources in India but in fact this is not what the paper is about. Still, one could cite the paper as an admonition to pay attention to the free troposphere when making simple interpretation of XCH<sub>4</sub>.

Response: The Indian region (South Asia in general) exerts a significant impact on the global CH<sub>4</sub> emissions. About 10% of total CH<sub>4</sub> emissions (550 Tg/yr) is emitted from the South Asian region (Patra et al., 2013). Investigations of sectoral emission of CH<sub>4</sub> over Indian region are thus significantly important, particularly over the Indo-Gangetic Plain (IGP) as the region is well-known hotspot of emissions of anthropogenic greenhouse gases. The transport mechanisms over the IGP and the Himalayan region are of global importance for transport and transformation of methane and other air pollutants; refer for example the aim of the SPARC/IGAC jointly sponsored activity - Atmospheric Composition and the Asian Monsoon (ACAM) project (<https://www2.acom.ucar.edu/acam>). It may also be pointed out here that there are several important projects being planned to achieve the ACAM goals (e.g., Stratospheric and upper tropospheric processes for better climate predictions; <http://www.stratoclim.org/>). Thus, we believe understanding the transport of CH<sub>4</sub> in one of the strongest monsoonal regions of the globe is not likely to be of a limited interest.

The space-based observations are limited to total columnar methane mixing ratios (XCH<sub>4</sub>). However, our knowledge of handling total column data in an inverse modelling system is limited and serious systematic biases require attention (e.g., Ostler et al., AMT, 2017). Thus, it is important to understand the source receptor relationships before inverse modeling of regional sources and sinks. Linking the surface emissions to the XCH<sub>4</sub> observations over the Indian region is not very straightforward because of the coexistence of deep convection and large emissions of CH<sub>4</sub> from a variety of both natural and anthropogenic sources. Therefore, recognizing the role of transport is extremely important in order to understand the contributions of emission signals to the XCH<sub>4</sub> variabilities.

We have revised manuscript text to clarify the aims of this manuscript in a significantly revised version. We would like to request the reviewer to take a look in to the revised version now uploaded.

The presentation of the paper could be improved to make it more attractive: the writing is fastidious with too much details, the grammar and style are often poor, the postage stamp figures scare the reader away (could you make do with fewer panels), and the math isn't clean.

Response: We apologize for the sloppiness in writing the submitted version. We have put our best effort in improving the presentation of text. We add or remove some unwanted and confusing text throughout the manuscript. The presentation of results and conclusion become now more clear and straightforward. We present the column calculation equation in Section 2.2 now in a simplistic way. A language editing service checked a preliminary version, but some late revisions did not go through the language check. Thank you very much for kindly providing us with quick comments.

We have improved presentations of all figures after readjusting and modifying the text fonts, axis label and titles etc as per the comments from both reviewers. Given below are some of the specifics:

Figure 1: We have changed labels and title font size in this revised figure.

Figure 2: We have also changed labels and title font size in this figure. We have removed the x-axis tick labels from top three rows, changed y-axis scale from 1760 to 1920 ppb, moved panel titles inside the panels and used that extra space to increase the panel size.

Figure 3: We have increased the font and label size, decoupled layer information from each panel, shifted this information to the rightmost part of panels, placed panel numbers at the top left corner of each panel, moved the stations name to the top side of plot and changed the aspect ratio of the revised figure.

Figure 4: We have increased the font and label size of this revised figure.

Figure 5: We have changed the fonts of all labeling, moved the panel title into the plot area with shaded (white) background, increased the length of tick marks, used the text “Vertical cross-sections” for left and middle column and “Horizontal cross section” for rightmost column on the top of figure, changed the color scale (new scale: 1750 – 1930 ppb) and shift the season names to the rightmost part of revised figure.

One minor thing: on line 42, delete “increase in”.

Response: The sentence has modified now in the revised manuscript.

#### References:

Patra, P. K., Canadell, J. G., Houghton, R. A., Piao, S. L., Oh, N.-H., Ciais, P., Manjunath, K. R., Chhabra, A., Wang, T., Bhattacharya, T., Bousquet, P., Hartman, J., Ito, A., Mayorga, E., Niwa, Y., Raymond, P. A., Sarma, V. V. S. S., and Lasco, R.: The carbon budget of South Asia, *Biogeosciences*, 10, 513-527, doi:10.5194/bg-10-513-2013, 2013.

Ostler, A., Sussmann, R., Patra, P. K., Houweling, S., De Bruine, M., Stiller, G. P., Haenel, F. J., Plieninger, J., Bousquet, P., Yin, Y., Saunio, M., Walker, K. A., Deutscher, N. M., Griffith, D. W. T., Blumenstock, T., Hase, F., Warneke, T., Wang, Z., Kivi, R., and Robinson, J.: Evaluation of column-averaged methane in models and TCCON with a focus on the stratosphere, *Atmos. Meas. Tech.*, 9, 4843-4859, doi:10.5194/amt-9-4843-2016, 2016.

**Reply to Anonymous Referee #2 (Received and published: 30 June 2017)**

## General comments:

The manuscript discusses the vertical distribution of tropospheric methane over South Asia based on ACTM calculations and GOSAT data. It is a valuable contribution for our understanding of transport and emission contributions to methane mixing ratios at different altitudes, in particular with regard to the influence of convection during the southwesterly summer monsoon.

Response: We thank the reviewer for careful evaluation and providing us feedback on the manuscript. We have revised the manuscript based on the general and specific comments from both of the reviewers. We have also worked very carefully on improving clarity of the manuscript text and figures. We hope the revised version is easy to follow the results and discussion of this study.

## Specific comments

The text is rather unstructured in some parts, such as subsections 3.1, 3.2 or the Conclusion sections) which makes it difficult to read. Having more paragraphs and using less abbreviation could easily improve this. Several times abbreviations are introduced which are not needed because the term does not get used frequently in the text (e.g. first line in abstract SLCF). The abbreviations used for the regions and for the pressure levels are not very intuitive. Abbreviations for the pressure levels may not be needed at all. The abstract is rather long and too detailed.

Response: We have revised the whole manuscript in accordance with your suggestions and the comments from Reviewer #1. The whole manuscript text has been revised significantly to the best of our ability. The abstract is made concise and straightforward. Hopefully, the meaning of the text is clearer and straightforward now.

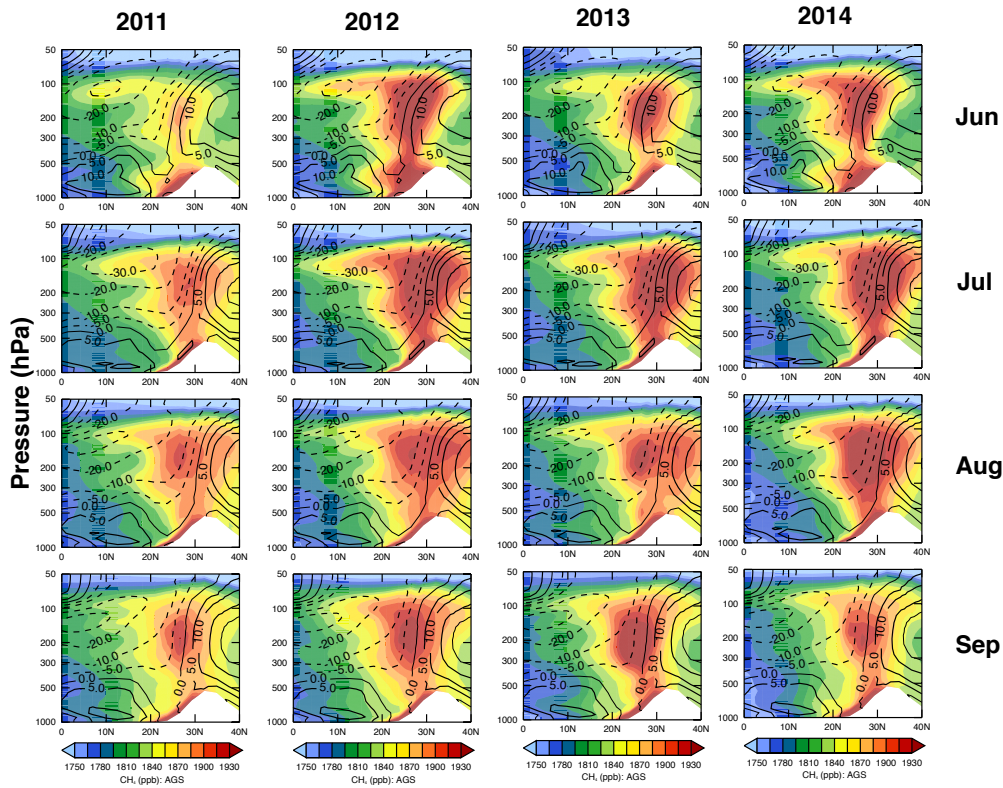
We tried to avoid the use of abbreviations as much as possible. As we stated in the text, the atmospheric column was segregated into five sigma-pressure ( $\sigma_p$ ) layers with an equal spacing of 0.2 starting from the surface level ( $\sigma_p=1$ ), corresponding to Lower Troposphere (LT), Mid-Troposphere1 (MT1), Mid-Troposphere2 (MT2), Upper Troposphere (UT) and Upper Atmosphere (UA), respectively. Those names are explicitly stated in the revised manuscript. To avoid using long names of those layers, we keep the abbreviations in the discussion.

The text uses sigma pressure level and pressure numbers in hPa interchangeably. This should be made consistent.

Response: The sigma pressure coordinate was used only to divide the atmospheric column into partial columns to avoid the effect of topography in the partial column calculations. In the later part on discussion, we used pressure numbers only.

I was wondering whether you checked if for the years studied here, namely 2011–2014, it was checked if the southwest monsoon fitted into the season scheme that was used here, i.e. was June truly a pre-monsoonal spring month in all four years and did the southwest monsoon prevail through September.

Response: Our main focus in this study is the analysis of mean features in XCH<sub>4</sub> seasonal cycle. To show the seasonal cycle clearly, we divided a year into four periods of 3 months duration, which is commonly used in meteorological studies (e.g., Rao, 1976). We repeated the analysis including June and excluding September from the southwest monsoon period, but didn't find significant difference that could affect our conclusion. To investigate the year-to-year variability of the period of the southwest monsoon season, we also individually plotted these transport processes for each year from 2011 to 2014 and didn't find any significant inter-annual variability in their nature. Please look at the following figure for reference. We have added this clarification in the main manuscript also.



Line 86 f



Here a contrast to the GOSAT TIR data is mentioned. This is not at all connected to the previous paragraph plus it has not yet been clearly stated that SWIR data is used in this manuscript. It does become later, though, but here the mentioning of the TIR data is confusing.

Response: Here the purpose of mentioning TIR band is just to provide information to readers about the availability of vertical CH<sub>4</sub> data, although they can't be used due to their limited validity in this study. This is the reason why we have to use the model simulations instead of the observation. But to avoid confusion we have removed the sentence in the revised manuscript.

Line 140

What does AGS stand for?

Response: Sorry for this confusion. AGS is not an abbreviation. AGS is a name of the ensemble emission dataset that is used in the ACTM as an a priori emission case. In this case the EDGAR4.2FT emissions from agricultural sectors are only allowed to change during the period of inversion (2001-2013), while all other anthropogenic emissions are kept constant at the 2002 level. Now we have modified the sentence in the following manner to make it clearer.

“The model sensitivity for emission is examined by two cases of emission scenarios based on different combination of sectoral emissions. First one is referred to the ‘AGS’, where all emission sectors in EDGAR42FT are kept at a constant value for 2000, except for emissions from agriculture soils. The second one is controlled emission scenario referred to ‘CTL’, which is based on the ensemble of the anthropogenic emissions from EDGAR32FT (as in Patra et al., 2011a), wetland and biomass burning emissions from Fung et al. (1991) and rice paddies emission from Yan et al. (2009)”.

Line 158 f.

It becomes obvious later in section 3.2. what you mean here, but on first reading it was totally unclear to me.

Response: We have removed this sentence from Section 2.2 and add a sentence in Section 3.2 in the revised manuscript to avoid the confusion.

“The partial columnar CH<sub>4</sub> are calculated within different  $\sigma_p$  layers (denoted by  $X_p\text{CH}_4$ ) using the same formula for  $X\text{CH}_4$ , as in Section 2.2.”

Line 165

What is the maximum spatial difference that will occur?

Response: The maximum spatial difference occurs about 1.2°.

Line 198 f.

I don't understand what was done here. How was the climatology in Figure S1 used for the data shown in Figure 2? Shouldn't it be the other way round, which Figure S1 shows the climatological means resulting from the time series shown in Figure 2?

Response: Sorry for the confusing sentence. Please read our modified sentence (lines 217-218) as:

“The monthly mean climatology, resulting from the time series shown in Figure 2, is shown in the supplementary information (Figure S1)”.

### Section 3.1

The discussion lacks a comparison between the GOSAT data and the ACTM results. In particular in June for EIGP, you discuss the difference in emission between the AGS and the CTL model run, but for both scenarios agreement with GOSAT looks rather poor compared to the other months. For arid India this holds also for July. This disagreement makes it difficult to discuss the difference between the model runs in great detail as none of them seem to reproduce the measurements very well.

Response: In Figure 3, there is a mismatch between ACTM emission scenarios and GOSAT observations in June for EIGP and also in some months for Arid India region. One possible reason is that there are not sufficient observations (less than 10 data) involved in the monthly mean corresponding to those months due to GOSAT sparseness in the coverage. However, despite the lack of data number in monsoon season, we can find both model scenarios are generally able to capture some of the available observations during the monsoon months in Figure 2. Here our main focus in comparison of GOSAT with ACTM is to confirm the ability of the model in producing the seasonal phase of XCH<sub>4</sub>. For these reasons, we do not discuss the discrepancy between GOSAT and ACTM in detail here.

Also, the monthly climatologies shown in Figure S1 have gaps that result from data lacking due to cloud cover. However, seasonalities shown in Figure 3, although based on the climatological means, do not show these gaps for the model data. So, was the treatment of the model data somehow different for this part of the study than for the previous one? I guess this is what you mean in Line 208 by 'without sampling'?

Response: In the revised manuscript we clearly stated that "climatology" means the monthly mean values for the period of 2011-2014 (see figure captions of Figure 3 and Figure S1 in the revised manuscript). Figure S1 shows the climatological monthly mean of all of the available GOSAT data. On the other hand, in Figure 1 and Figure 2, we have sampled the model data that are collocated and coincident with GOSAT observations. In Figure 3, we included all of the model data in the panels of three selected regions (a6, b6, and c6) to show the seasonal cycle clearly.

Wording

Line 54

'which could fill in gap' does not make sense.

Response: We have modified the sentence to:

"Recent technological advances have made it possible to detect spatial and temporal variations in atmospheric CH<sub>4</sub> from space (Frankenberg et al., 2008; Kuze et al., 2009), which could provide global and dense data over the regions uncovered by ground, aircraft and ship-based measurements, albeit at a lower accuracy than the *in situ* measurements."

Line 60 f.

'The Indo-Gangetic Plane ... Himalayas' — The wording here does not make sense.

Response: We have modified this sentence in the revised manuscript.

"The Indo-Gangetic Plain (IGP) located in the foothills of the Himalayas is one of the most polluted regions in the world, which hosts 70% of coal-fired thermal power plants in India and experiences intense agricultural activity".

Line 68

It's either convection or convective uplift but not convection uplift.

Response: We have modified this sentence in the revised manuscript.

" Rainfall during the SW monsoon season cause higher CH<sub>4</sub> emissions from the paddy fields and wetlands while the persistent deep convection results the updraft of CH<sub>4</sub>-laden air mass from the surface to the upper troposphere during the same season, which is then confined by anticyclonic winds at the this height."

Line 71

Typo in 'plateau'.

Response: Corrected.

Line 77

'related the high XCH<sub>4</sub> values correspond' does not make sense.

Response: We have modified the sentence to:

"Previous studies have linked these high XCH<sub>4</sub> levels to the strong surface CH<sub>4</sub> emissions particularly from the rice cultivation over the Indian region, because they showed statistically significant correlations over certain regions."

Line 81

What do you mean by 'inferring the local emissions to the higher emissions'?

Response: Here we want to mention that high XCH<sub>4</sub> cannot be directly linked with high local/regional emissions. We have changed the sentence for better clarity to:

“However, inferring local emissions directly from variations in XCH<sub>4</sub> is ambiguous particularly over the Indian regions under the influence of monsoon meteorology, because XCH<sub>4</sub> involves contributions of CH<sub>4</sub> abundances from all altitudes along the solar light path.”

Line 86 f

Grammar in this sentence is not logical.

Response: This sentence has been removed from the revised version as per your suggestion.

Line 92 f

‘under the limitations of satellite’ — Please re-formulate.

Response: This sentence has been removed from the revised version.

Line 142

change ‘kept at constant at a value’ to ‘kept at a constant value’

Response: Changed

Line 156

Why is there an ‘and’ here?

Response: Sorry for this typo error. We have removed ‘and’ in the revised manuscript.

Line 223/224

‘will equally applicable’ does not make sense.

Response: This sentence is eliminated in the revised version.

Line 320

‘we have been observed’ does not make sense.

Response: We have modified the sentence in the revised manuscript.

“We have shown that the distinct spatial and temporal variations of XCH<sub>4</sub> observed by GOSAT are not only governed by the heterogeneity in surface emissions but also due to complex atmospheric transport mechanisms caused by the seasonally varying Asian monsoon.”

Line 333/334

Grammar is not logical here

Response: We have modified the sentence in the revised manuscript.

“The persistent deep convection during the southwest monsoon season (June-August) causes strong updrafts of CH<sub>4</sub>-rich air mass from the surface to upper tropospheric heights (~200 hPa), which is then confined by anticyclonic winds at this height. The anticyclonic confinement of surface emission over a wider South Asia region leads to strong contribution of the upper troposphere in formation of the XCH<sub>4</sub> peak over most regions in northern India, including the semi-arid regions with extremely low CH<sub>4</sub> emissions.”

## Figures and Tables

In general, most figures are too small and use too small fonts for labels and annotations, in particular axis labels. Panel labels a, b, c ... are very difficult to spot, which makes it complicate to follow the discussion in the text.

Response: We apologize for this. We have improved presentations of all figures after readjusting and modifying the text fonts, axis label and titles etc. Given below are some of the specifics:

Figure 1: We have changed labels and title font size in this revised figure.

Figure 2: We have also changed labels and title font size in this figure. We have removed the x-axis tick labels from top three rows, changed y-axis scale from 1760 to 1920 ppb, moved panel titles inside the panels and used that extra space to increase the panel size.

Figure 3: We have increased the font and label size, decoupled layer information from each panel, shifted this information to the rightmost part of panels, placed panel numbers at the top left corner of each panel, moved the stations name to the top side of plot and changed the aspect ratio of the revised figure.

Figure 4: We have increased the font and label size of this revised figure.

Figure 5: We have changed the fonts of all labeling, moved the panel title into the plot area with shaded (white) background, increased the length of tick marks, used the text “Vertical cross-sections” for left and middle column and “Horizontal cross section” for rightmost column on the top of figure, changed the color scale (new scale: 1750 – 1930 ppb) and shift the season names to the rightmost part of revised figure.

### Figure 2

This figure has too many panels resulting in them being too small. Think about separating the map into a decently sized figure on its own and presenting panels b–l in a classical two-column scheme with larger panels.

Response: We increased the area within each panels after readjusting the fonts of labels and moving the panel title within the plot area. We want to show the regions in India map and XCH<sub>4</sub> variability over those regions together and thus we prefer to keep the arrangement of the panels as before. We think this arrangement will be convenient for the reader to track the location and XCH<sub>4</sub> distribution in the same figure.

### Figure 5

Y-axis has no label and no units.

Response. We have added the label for Y-axis.

### Figure 5

Caption: change 'year of 2011' to 'year 2011'.

Response: Changed

### Table S1

Table says 'South India' but 'Southern Peninsula' is used throughout the text. Think about also including the abbreviations for the regions used in the text into the table.

**Response:** Changed

# 1 What controls the seasonal cycle of columnar methane observed by 2 GOSAT over different regions in India?

3 Naveen Chandra<sup>1\*</sup>, Sachiko Hayashida<sup>1</sup>, Tazu Saeki<sup>2</sup>, and Prabir K. Patra<sup>2</sup>

4  
5 <sup>1</sup> Nara Women's University, Kita-Uoya Nishimachi, Nara 630-8506, Japan

6 <sup>2</sup> Department of Environmental Geochemical Cycle Research, JAMSTEC, Yokohama 2360001, Japan

7  
8 Correspondence to: Naveen Chandra ([nav.phy09@gmail.com](mailto:nav.phy09@gmail.com))

9  
10 **Abstract.** Methane (CH<sub>4</sub>) is one of the most important short-lived climate forcings for its critical roles in greenhouse warming and  
11 air pollution chemistry in the troposphere, and water vapor budget in the stratosphere. It is estimated that up to about 8% of  
12 global CH<sub>4</sub> emissions occur from South Asia, covering less than 1% of the global land. With the availability of satellite  
13 observations from space, variability in CH<sub>4</sub> have been captured for most parts of the global land with major emissions, which  
14 were otherwise not covered by the surface observation network. The satellite observation of the columnar dry-air mole fractions  
15 of methane (XCH<sub>4</sub>) is an integrated measure of CH<sub>4</sub> densities at all altitudes from the surface to the top of the atmosphere. Here,  
16 we present an analysis of XCH<sub>4</sub> variability over different parts of India and the surrounding cleaner oceanic regions of India as  
17 measured by the Greenhouse gases Observation SATellite (GOSAT), and simulated by an atmospheric chemistry-transport model  
18 (ACTM). Distinct seasonal variations of XCH<sub>4</sub> have been observed over the northern (north of 15°N) and the southern part  
19 (south of 15°N) of India, corresponding to the peak during southwest monsoon (July-September) and early autumn season  
20 (October-December), respectively. Analysis of the transport, emission and chemistry contributions to XCH<sub>4</sub> using ACTM  
21 suggests that distinct XCH<sub>4</sub> seasonal cycle over northern and southern regions of India is governed by both heterogeneous  
22 distributions of surface emissions, and contribution of the partial CH<sub>4</sub> column in the upper troposphere. Over most part of the  
23 northern Indian Gangetic Plain regions, up to 40% of the peak-to-trough amplitude during the southwest (SW) monsoon season  
24 is attributed to the lower troposphere (~1000-600 hPa), while ~40% to uplifted high-CH<sub>4</sub> air masses in the upper troposphere  
25 (~600-200 hPa). In contrast, the XCH<sub>4</sub> seasonal enhancement over the semi-arid western India is attributed mainly (~70%) to the  
26 upper troposphere. The lower tropospheric region contributes up to 60% in the XCH<sub>4</sub> seasonal enhancement over the southern  
27 peninsula and oceanic region. These differences arise due to the complex atmospheric transport mechanisms, caused by the  
28 seasonally varying monsoon. The CH<sub>4</sub> enriched air mass is uplifted from high emission region of the Gangetic Plain by the SW  
29 monsoon circulation and deep cumulus convection, and then confined by anticyclonic wind in the upper tropospheric heights  
30 (~200 hPa). The anticyclonic confinement of surface emission over a wider South Asia region leads to strong contribution of the  
31 upper troposphere in the formation of the XCH<sub>4</sub> peak over northern India, including the semi-arid regions with extremely low  
32 CH<sub>4</sub> emissions. Based on this analysis, we suggest that a link between surface emissions and higher levels of XCH<sub>4</sub> is not always  
33 valid over Asian monsoon regions, although there is often a fair correlation between surface emissions and XCH<sub>4</sub>. The overall  
34 validity of ACTM simulation for capturing GOSAT observed seasonal and spatial XCH<sub>4</sub> variability will allow us to perform  
35 inverse modelling of XCH<sub>4</sub> emissions in the future using XCH<sub>4</sub> data.

36

Deleted: (SLCFs)

林田佐智子 6/21/2017 3:37 PM

Deleted: according to the United Nation ... [1]

Prabir Patra 6/19/2017 10:43 AM

Deleted: as well as it plays also a

林田佐智子 6/21/2017 3:38 PM

Deleted: u... budget in the stratosphere. ... [2]

Naveen Negi 7/3/2017 10:17 AM

Deleted: The ... he satellite observation ... [3]

林田佐智子 6/21/2017 3:42 PM

Deleted: along the solar light path betwe ... [4]

Prabir Patra 6/19/2017 10:48 AM

Deleted: Observations of enhanced XCI ... [5]

林田佐智子 6/21/2017 3:42 PM

Deleted: ies

Prabir Patra 6/19/2017 10:50 AM

Deleted: y

Naveen Negi 7/3/2017 10:19 AM

Deleted: different inland and

Prabir Patra 6/19/2017 10:50 AM

Deleted: using ... s measured by the ... [6]

林田佐智子 6/21/2017 3:48 PM

Deleted:

Prabir Patra 6/21/2017 10:14 PM

Deleted: located in ... the northern (north ... [7]

Naveen Negi 7/3/2017 1:06 PM

Formatted ... [8]

Naveen Negi 6/22/2017 10:55 AM

Deleted: o

Naveen Negi 7/3/2017 1:06 PM

Formatted ... [9]

Naveen Negi 6/22/2017 10:55 AM

Deleted: 2

林田佐智子 6/21/2017 3:48 PM

Formatted ... [10]

Prabir Patra 6/19/2017 10:54 AM

Deleted: ) responsible for XCH<sub>4</sub> season ... [11]

Naveen Negi 7/3/2017 10:25 AM

Deleted: the

Prabir Patra 6/19/2017 10:55 AM

Deleted: , but also distribution of ... and ... [12]

Naveen Negi 8/14/2017 1:09 PM

Deleted: peak... eak-to-trough amplitud ... [13]

Prabir Patra 6/19/2017 10:59 AM

Deleted: atmosphere

Naveen Negi 6/22/2017 11:07 AM

Deleted: 88%

Prabir Patra 6/19/2017 11:00 AM

Deleted: attributed ... o the upper atmo ... [14]

Naveen Negi 7/20/2017 11:10 AM

Deleted: is contributed up to 60% by t ... [15]

Prabir Patra 6/19/2017 11:02 AM

Deleted: es

Naveen Negi 7/31/2017 4:07 PM

Deleted: ,

Prabir Patra 6/19/2017 11:02 AM

Deleted: e... heights (~200 hPa). The ... [16]

Naveen Negi 8/14/2017 1:08 PM

Deleted: most of the regions lying in

Prabir Patra 6/19/2017 11:09 AM

... [17]

Naveen Negi 7/3/2017 10:36 AM

Moved (insertion) [1]

Naveen Negi 7/3/2017 10:36 AM

... [19]

## 1. Introduction

Methane (CH<sub>4</sub>) is the second most important anthropogenic greenhouse gas (GHG) after carbon dioxide (CO<sub>2</sub>) and accounts for ~20% (+0.97 W m<sup>-2</sup>) of the increase in total direct radiative forcing, since 1750 (Myhre et al., 2013). CH<sub>4</sub> is emitted from a range of anthropogenic and natural sources on the Earth's surface into the atmosphere. The main natural sources of CH<sub>4</sub> include wetlands and termites (Matthews and Fung, 1987; Cao et al., 1998; Sugimoto et al., 1998). Livestock, rice cultivation, fossil fuel industry (production and uses of natural gas, oil and coal) and landfills are the major sectors among the anthropogenic sources (Crutzen et al., 1986; Minami and Neue, 1994; Olivier et al., 2006). These results also suggest that the Asian region is emission hotspot of CH<sub>4</sub> due to the large number livestock, intense cultivation, coal mining, waste management and other anthropogenic activities (EDGAR2FT, 2013).

With a short atmospheric lifetime of about 10 years (e.g., Patra et al., 2011a) and having 34 times more potential to trap heat than CO<sub>2</sub> on mass basis over a 100-year timescale (Gillett and Matthews, 2010, Myhre et al., 2013), mitigation of CH<sub>4</sub> emissions could be the most important way to limit global warming at inter-decadal time scales (Shindell et al., 2009). Better knowledge of CH<sub>4</sub> distribution and quantification of its emission flux is indispensable for assessing possible mitigation strategies. However, sources of CH<sub>4</sub> are not yet well quantified due to sparse ground based measurements, which results in limited representation of CH<sub>4</sub> flux on a larger scale (Dlugokencky et al., 2011; Patra et al., 2016). Recent technological advances have made it possible to detect spatial and temporal variations in atmospheric CH<sub>4</sub> from space (Frankenberg et al., 2005; Kuze et al., 2009), which could fill the gaps left by ground, aircraft and ship-based measurements, albeit at a lower accuracy than the in situ measurements. Further, despite the satellite observations having an advantage of providing continuous monitoring over a wide spatial range, the information obtained from passive nadir-sensors that use solar radiation at Short-Wavelength Infrared (SWIR) spectral band, is limited to columnar dry-air mole fractions of methane (XCH<sub>4</sub>). This is an integrated measure of CH<sub>4</sub> with contributions from the different vertical atmospheric layers, i.e., from the measurement point on the Earth's surface to the top of the atmosphere (up to about 100km, or more precisely to the satellite orbit).

The South Asia region, consisting of India, Pakistan, Bangladesh, Nepal, Bhutan and Sri Lanka, exerts a significant impact on the global CH<sub>4</sub> emissions, with regional total emissions of 37±3.7 Tg-CH<sub>4</sub> of about 500 Tg-CH<sub>4</sub> global total emissions during the 2000s (Patra et al., 2013). The Indo-Gangetic Plain (IGP) located in the foothills of the Himalayas is one of the most polluted regions in the world, which hosts 70% of coal-fired thermal power plants in India and experiences intense agricultural activity (Kar et al., 2010). This region is of particular interest mainly due to the coexistence of deep convection and large emission of pollutants (including CH<sub>4</sub>) from a variety of natural and anthropogenic sources. Rainfall during the SW monsoon season cause higher CH<sub>4</sub> emissions from the paddy fields and wetlands (e.g., Matthews and Fung, 1987; Yan et al., 2009; Hayashida et al., 2013) while the persistent deep convection results the updraft of CH<sub>4</sub>-laden air mass from the surface to the upper troposphere during the same season, which is then confined by anticyclonic winds at the this height (Patra et al., 2011b; Baker et al., 2012; Schuck et al., 2012). Several other studies also have highlighted the role of convective transport of pollutants (including CH<sub>4</sub>) from surface to the upper troposphere (400 – 200 hPa) during SW monsoon season (July-September) (Park et al., 2004; Randel et al., 2006; Xiong et al., 2009; Lal et al., 2014, Chandra et al., 2016). The dynamical system dominated by deep convection and anticyclone cover mostly the northern Indian region (north of 15°N) due to the presence of the Himalayas and the Tibetan Plateau, while such complex dynamical system has not been observed over the southern part of India (south of 15°N) (Rao, 1976).

Naveen Negi 7/3/2017 10:37 AM

Deleted: ally produced

林田佐智子 6/21/2017 4:00 PM

Deleted:

Prabir Patra 6/19/2017 12:02 PM

Deleted: ; EDGAR2FT, 2013

Naveen Negi 6/23/2017 11:52 AM

Deleted: per molecule

Naveen Negi 7/3/2017 10:46 AM

Formatted: Not Highlight

Naveen Negi 8/14/2017 1:15 AM

Deleted: IPCC AR5

Naveen Negi 8/14/2017 1:11 PM

Formatted: Subscript

Naveen Negi 7/3/2017 10:42 AM

Deleted: in

Naveen Negi 7/3/2017 10:44 AM

Deleted: -based

Prabir Patra 6/19/2017 11:46 AM

Deleted: Although

Prabir Patra 6/19/2017 11:58 AM

Deleted: c

Prabir Patra 6/19/2017 11:46 AM

Deleted: the

Naveen Negi 7/3/2017 10:44 AM

Deleted: region

Prabir Patra 6/19/2017 11:59 AM

Deleted: .

林田佐智子 6/21/2017 4:13 PM

Deleted: for molecular CH<sub>4</sub>)

Prabir Patra 6/19/2017 11:48 AM

Formatted: Subscript



Satellite-based measurements show elevated levels of XCH<sub>4</sub> over the northern part of India (north of 15°N) particularly high over IGP during the SW monsoon season (July to September) and over southern India (south of 15°N) during early autumn season (October to December) (Frankenberg et al., 2008, 2011; Hayashida et al., 2013). Previous studies have linked these high XCH<sub>4</sub> levels to the strong surface CH<sub>4</sub> emissions particularly from the rice cultivation over the Indian region, because they showed statistically significant correlations over certain regions (Hayashida et al., 2013; Kavitha et al., 2016). The differences in the peak of XCH<sub>4</sub> seasonal cycle over northern and southern regions of India are also discussed on the basis of agricultural practice in India that takes place in two seasons, May to October, and November to April, respectively. However, inferring local emissions directly from variations in XCH<sub>4</sub> is ambiguous, particularly over the Indian regions under the influence of monsoon meteorology, because XCH<sub>4</sub> involves contributions of CH<sub>3</sub> abundances from all altitudes along the solar light path.

This study attempts for the first time to separate the factors responsible (emission, transport and chemistry) for the distributions of columnar methane (XCH<sub>4</sub>) over the Asian monsoon region for different altitude segments. The XCH<sub>4</sub> mixing ratios are used for this study as observed from the GOSAT and simulated by JAMSTEC's ACTM. We aim to understand relative contributions of surface emissions and transport in the formation of XCH<sub>4</sub> seasonal cycles over different parts of India and the surrounding oceans. This understanding will help us in developing an inverse modelling system for estimation of CH<sub>4</sub> surface emissions using XCH<sub>4</sub> observations and ACTM forward simulation.

## 2. Methods

### 2.1 Satellite data:

The Greenhouse gases Observing SATellite (GOSAT) (also referred to as Ibuki) is a joint satellite project is developed jointly by the National Institute for Environmental Studies (NIES), Ministry of the Environment (MOE) and Japan Aerospace Exploration Agency (JAXA). It has been providing columnar dry air mole fractions of the two important greenhouse gases (XCH<sub>4</sub> and XCO<sub>2</sub>) at near global coverage since its launch in January 2009. It is equipped onboard with the Thermal And Near infrared Sensor for carbon Observation-Fourier Transform Spectrometer (TANSO-FTS) and the Cloud and Aerosol Imager (TANSO-CAI) (Kuze et al., 2009). To avoid cloud contamination in the retrieval process, any scene with more than one cloudy pixel within the TANSO-FTS IFOV is excluded. The atmospheric images from CAI are used to identify the cloudy pixels. As a result of this strict screening, only limited numbers of XCH<sub>4</sub> data are available during the SW monsoon over South Asia. This study uses the GOSAT SWIR XCH<sub>4</sub> (Version 2.21)-Research Announcement product for the period of 2011-2014. The ground-based FTS measurements of XCH<sub>4</sub> by the Total Carbon Column Observing Network (TCCON) (Wunch et al., 2011) are used extensively to validate the GOSAT retrievals. Retrieval bias and precision of column abundance from GOSAT SWIR observations have been estimated as approximately 15-20 ppb and 1%, respectively for the NIES product using TCCON data (Morino et al., 2011; Yoshida et al., 2013).

### 2.2. Model simulations

Model analysis is comprised of simulations from the JAMSTEC's atmospheric general circulation model (AGCM)-based chemistry-transport model (ACTM; Patra et al., 2009). The AGCM was developed by the Center for Climate System Research/National Institute for Environmental Studies/Frontier Research Center for Global Change (CCSR/NIES/FRCGC). It has been parts of the transport model inter-comparison experiment TransCom-CH<sub>4</sub> (Patra et al., 2011a) and used in inverse

Naveen Negi 7/3/2017 10:42 AM

Deleted: The Indian region exerts a significant impact on the global CH<sub>4</sub> emissions (Patra et al., 2013). The Indo-Gangetic Plain (IGP), mostly hot and humid northeast region lies in the foothills of the Himalayas, is one of [20]

林田佐智子 6/21/2017 4:16 PM

Deleted: season ... Frankenberg et al., [21]

Naveen Negi 7/3/2017 11:03 AM

Deleted: related ... ave linked these hig [22]

林田佐智子 6/21/2017 4:26 PM

Deleted: namely the Kharif ... ay to [23]

Prabir Patra 6/19/2017 12:25 PM

Deleted: the ... local emissions to the hi [24]

Naveen Negi 7/3/2017 11:05 AM

Deleted: because XCH<sub>4</sub>, which involve [25]

Prabir Patra 6/19/2017 12:27 PM

Deleted: is highly ambiguous, ... articu [26]

Naveen Negi 7/31/2017 4:07 PM

Deleted: . Therefore, data indicating th [27]

Prabir Patra 6/19/2017 12:35 PM

Deleted: Some studies have been done [28]

Naveen Negi 7/3/2017 11:07 AM

Deleted: manuscript ... study attempts fo [29]

Naveen Negi 8/14/2017 1:11 PM

Deleted: We aim to understand relative [30]

Prabir Patra 6/19/2017 12:41 PM

Deleted: called

Naveen Negi 8/14/2017 1:12 PM

Deleted: of ... the National Institute for [31]

Prabir Patra 6/19/2017 12:42 PM

Deleted: global observations of ... olun [32]

Naveen Negi 7/3/2017 11:29 AM

Deleted: with onboard the

林田佐智子 6/21/2017 4:41 PM

Deleted: thermal and near infrared sens [33]

Prabir Patra 6/21/2017 10:19 PM

Deleted: is removed if ... ith more than [34]

Naveen Negi 6/22/2017 11:13 AM

Deleted: The cloudy pixels are identifi [35]

林田佐智子 6/21/2017 4:50 PM

Deleted: Cloudy data is strictly screenc [36]

Naveen Negi 7/3/2017 11:30 AM

Deleted: season ... ver South Asia. This [37]

Prabir Patra 6/19/2017 12:47 PM

Deleted: ... obtained using the worldw [38]

Prabir Patra 6/19/2017 1:43 PM

Deleted: well-established

Naveen Negi 7/31/2017 4:08 PM

Deleted: a

Prabir Patra 6/19/2017 1:44 PM

Deleted: chemistry-

488 modeling of CH<sub>4</sub> emissions from in situ observations (Patra et al., 2016). The ACTM runs at a horizontal resolution of T42  
 489 spectral truncations (~2.8° × 2.8°) with 67 sigma-pressure vertical levels. The evolution of CH<sub>4</sub> at different longitude (x),  
 490 latitude (y) and altitude (z) with time in the Earth's atmosphere depends on the surface emission, chemical loss and transport,  
 491 which can be mathematically represented by the following continuity equation:  
 492

$$\frac{dCH_4(x,y,z,t)}{dt} = S_{CH_4}(x,y,t) - L_{CH_4}(x,y,z,t) - \nabla \cdot \phi(x,y,z,t)$$

493 where

494 CH<sub>4</sub> = methane burden in the atmosphere

495 S<sub>CH<sub>4</sub></sub> = Total emissions/sinks of CH<sub>4</sub> at the surface

496 L<sub>CH<sub>4</sub></sub> = Total loss of CH<sub>4</sub> in the atmosphere due to the chemical reactions

497 ∇ · φ = Transport of CH<sub>4</sub> due to the advection, convection and diffusion.

498

499 The meteorological fields of ACTM are nudged with reanalysis data from the Japan Meteorological Agency, version JRA-25  
 500 (Onogi et al., 2007). The model uses an optimal OH field (Patra et al., 2014) based on a scaled version of the seasonally varying  
 501 OH field (Spivakovsky et al., 2000). The a priori anthropogenic emissions are from Emission Database for Global Atmospheric  
 502 Research (EDGAR) v4.2 FT2010 database (<http://edgar.jrc.ec.europa.eu>). The model sensitivity for emission is examined by  
 503 two cases of emission scenarios based on different combination of sectoral emissions. First one referred to the 'AGS', where all  
 504 emission sectors in EDGAR42FT are kept a constant value for 2000, except for emissions from agriculture soils. The second one  
 505 is controlled emission scenario referred to 'CTL', which is based on the ensemble of the anthropogenic emissions from  
 506 EDGAR32FT (as in Patra et al., 2011a), wetland and biomass burning emissions from Fung et al (1991) and rice paddies  
 507 emission from Yan et al (2009). The emission seasonality differs substantially between the CTL case and the AGS case due to  
 508 differences in emissions from wetlands, rice paddies and biomass burning; other anthropogenic emissions do not contain  
 509 seasonal variations (Patra et al., 2016). Further details about the model and these emission scenarios can be found in the previous  
 510 studies (Patra et al., 2009; Patra et al., 2011a; Patra et al., 2016).

511 XCH<sub>4</sub> is calculated from the ACTM profile using following equations:

$$512 XCH_4 = \sum_{n=1}^{60} CH_4(n) \times \Delta\sigma_p(n)$$

513 where, CH<sub>4</sub>(n) is the dry-air mole fraction at model mid-point level, n = number of vertical sigma pressure layers of ACTM (=  
 514 1-60 with σ<sub>p</sub> values of 1.0 and 0.005), Δσ<sub>p</sub> = thickness of sigma pressure level. Note here that we have not incorporated  
 515 convolution of model profiles with retrieval a priori and averaging kernels. Because the averaging kernels are nearly constant in  
 516 the troposphere (Yoshida et al., 2011), hence this approximation does not lead to serious errors in constructing the model XCH<sub>4</sub>.

517 For both the CTL and AGS cases, we adjust a constant offset of 20 ppb to the modeled time series, which should make the *a*  
 518 *priori* correction have a lesser impact on the model XCH<sub>4</sub>. Because the focus of this study is seasonal and spatial variations in  
 519 XCH<sub>4</sub>, a constant offset adjustment should not affect the main conclusions.

520

### 521 3. Results and discussion

#### 522 3.1 XCH<sub>4</sub> over the Indian region: View from GOSAT and ACTM simulations

523 This section presents an analysis of XCH<sub>4</sub> observed by GOSAT from Jan 2011 to Dec 2014 over the Indian region. We  
 524

Deleted: and...mathematically can be ... [39]

Naveen Negi 8/14/2017 1:14 AM

Deleted: molar fraction in

Prabir Patra 6/19/2017 1:45 PM

Deleted: optimized ...ptimal OH field ... [40]

林田佐智子 6/23/2017 12:08 PM

Comment [1]: I cannot follow the sent ... [45]

Naveen Negi 6/22/2017 11:30 AM

Deleted: T...o different ...ases of emis ... [41]

Naveen Negi 7/3/2017 11:33 AM

Deleted: is the ACTM...eferred to th ... [46]

林田佐智子 6/21/2017 5:46 PM

Formatted ... [42]

Prabir Patra 6/21/2017 10:22 PM

Formatted ... [43]

林田佐智子 6/21/2017 5:46 PM

Formatted ... [44]

林田佐智子 6/21/2017 5:48 PM

Comment [2]: Seasonality in emission ... [47]

Prabir Patra 6/19/2017 1:46 PM

Deleted: the...following ... [48]

Prabir Patra 6/19/2017 1:47 PM

Deleted: γ<sup>-0</sup> CH<sub>4</sub> (n) X\* ...Δ [(...)<sub>p</sub> (n) ... [49]

Prabir Patra 6/19/2017 1:49 PM

Deleted: For the first layer (n = 1) - ... [50]

Naveen Negi 7/31/2017 4:10 PM

Deleted: s...gma pressure level. Note h ... [51]

Prabir Patra 6/23/2017 12:11 PM

Comment [3]: Check and give an accur ... [54]

Prabir Patra 6/23/2017 1:04 PM

Comment [4]: DID YOU CHECK???

Prabir Patra 6/23/2017 1:05 PM

Formatted ... [53]

Prabir Patra 6/23/2017 1:05 PM

Formatted ... [55]

Prabir Patra 6/23/2017 1:05 PM

Formatted ... [56]

Prabir Patra 6/19/2017 2:00 PM

Moved (insertion) [2] ... [57]

Prabir Patra 6/19/2017 2:00 PM

Deleted: (AKs)

Naveen Negi 7/3/2017 11:35 AM

Deleted: uniform

林田佐智子 6/21/2017 4:52 PM

Formatted ... [52]

林田佐智子 6/21/2017 4:52 PM

Deleted: 3

Prabir Patra 6/19/2017 2:01 PM

Deleted: and X<sub>p</sub>CH<sub>4</sub> in the tropical reg... [58]

Naveen Negi 7/31/2017 4:10 PM

Deleted: The seasonal distributions of ... [59]

Prabir Patra 6/19/2017 2:00 PM

Moved up [2]: Because the averaging l... [60]

Naveen Negi 7/31/2017 4:11 PM

Deleted: XCH<sub>4</sub> data are sampled at the ... [61]

Naveen Negi 8/8/2017 12:14 AM

Deleted: -

Prabir Patra 6/19/2017 2:09 PM

Deleted: mixing ratios

Naveen Negi 8/8/2017 12:14 AM

... [62]

Prabir Patra 6/19/2017 2:04 PM

... [63]

characterize the 4 seasons specific to the region as winter (January to March), spring (April to June), summer (July to September) or the SW monsoon, and autumn (October to December) as commonly used in meteorological studies (e.g., Rao, 1976). To study the seasonal  $XCH_4$  pattern in details depending on the distinct spatial pattern of surface emissions and  $XCH_4$  mixing ratios shown in Figure 1, the Indian landmass was partitioned into eight sub-regions: Northeast India (NEI), Eastern India (EI), Eastern IGP (EIGP), Western IGP (WIGP), Central India (CI), Arid India (AI), Western India (WI), Southern Peninsula (SP), and two surrounding oceanic regions, the Arabian Sea (AS) and Bay of Bengal (BOB) (Figure 2a). Regional divisions are made based on spatial patterns of emission and  $XCH_4$  (Figure 1a1-c2), and our knowledge of seasonal meteorological conditions. Since general features of  $XCH_4$  simulated by ACTM using emission scenarios AGS and CTL are similar to each other, the main discussion is made using AGS scenario only.

Figure 1a1-a2 show that the  $XCH_4$  mixing ratios are lower in spring season and higher in autumn. A strong latitudinal gradient in  $XCH_4$  is observed between the Indo-Gangetic Plain (IGP) and the other parts of India.  $XCH_4$  show the highest value (~1880 ppb) over the IGP, eastern and northeast Indian regions. As seen from Figure 1b1-b2, ACTM simulations are able to reproduce the observed latitudinal and seasonal gradients in  $XCH_4$ ; i.e., higher values during the southwest monsoon and autumn seasons and lower values during the winter and spring seasons over the IGP region. The optimized total  $CH_4$  fluxes (AGS and CTL) show high emissions over the IGP region and northeast Indian regions (Figure 1c1-c2). Most elevated levels of  $XCH_4$  are often observed simultaneously with the higher emissions, suggesting a link between the enhanced  $XCH_4$  and high surface emissions in summer (not shown in Figure 1). However, this link is not valid for all locations. For example, over the western and southern region of India,  $XCH_4$  is higher in autumn than in spring, though the emissions are higher in spring.

Figure 2b-k shows ACTM - GOSAT comparisons of  $XCH_4$  time series from Jan 2011 to Dec 2014 over the selected study regions. The simulated  $XCH_4$  data are sampled at the nearest model grid to the available GOSAT observations and at the satellite overpass time (~ 1300 LT) and then averaged over each study region. Observations are sparse or not available during the SW monsoon season in some of the regions due to limitations of GOSAT retrieval under cloud cover. The model captures the salient features of the seasonal cycles at very high statistical significance (correlation coefficients,  $r > 0.8$ ; except for NE India; Table 1) over the selected regions (refer to Table 1). The high ACTM-GOSAT correlations for the low/no emission regions suggest that transport and chemistry are accurately modeled in ACTM. Although we do not have the statistically significant number of observations for the SW monsoon period, the observed high GOSAT  $XCH_4$  are generally well simulated by ACTM over most of the study regions. Based on these comparisons, we can assume that model simulations can be used to understand  $XCH_4$  variability over the Indian region. Though we showed only the paired GOSAT and ACTM data that matched in time and location in Figure 2b-k, we also confirmed that the correlation is high ( $r \sim 0.9$ ) between the monthly-averaged time series of GOSAT and ACTM averaged for the four years (2011-2014) when ACTM is not co-sampled at the GOSAT sampling points (Figure S1). These high correlations assure representativeness of the data shown in Figure 2b-k. Thus, the seasonal evolution of  $XCH_4$  using the ACTM simulations alone is expected to be fairly valid for different altitude layers (ref. to Patra et al., 2011b for comparison at the aircraft cruising altitude). Though the model is only validated for  $XCH_4$  in this study, comparisons with surface and independent aircraft  $CH_4$  observations have been shown in Patra et al. (2016).

Naveen Negi 8/14/2017 1:13 AM

**Deleted:** We characterize the 4 seasons specific to the regional mean from January to March as "wWinter" (January to March), April to June as "Sspring (April to June)", summer (July to September as "Summer" or the southwest summer monsoon" and autumn (October to December as "Autumn"); this nomenclature is maintained throughout ... [64]

Naveen Negi 8/14/2017 1:13 AM

**Deleted:** Since general features of XCH<sub>4</sub> ... [65]

Naveen Negi 7/20/2017 3:46 PM

**Deleted:** b...1a-b ... [66]

Prabir Patra 6/19/2017 2:11 PM

**Deleted:** the observed  $XCH_4$  variation f... [67]

Naveen Negi 7/31/2017 4:20 PM

**Deleted:** during the ... [68]

Prabir Patra 6/19/2017 2:11 PM

**Deleted:** s ... [69]

Naveen Negi 7/31/2017 4:20 PM

**Deleted:** during ...n the ...utumn seas... [68]

Prabir Patra 6/19/2017 2:11 PM

**Deleted:** s... A strong latitudinal gradi... [69]

Naveen Negi 7/3/2017 11:40 AM

**Deleted:** remainder ... [70]

Prabir Patra 6/19/2017 2:13 PM

**Deleted:** mixing ratios ...how the high... [70]

Naveen Negi 7/20/2017 3:46 PM

**Deleted:** c...b21c-d ... [71]

Prabir Patra 6/19/2017 2:13 PM

**Deleted:** mixing ratio...alues during th... [72]

Naveen Negi 6/22/2017 11:50 AM

**Deleted:** shows ... [73]

Prabir Patra 6/19/2017 2:16 PM

**Deleted:** the ... [74]

Naveen Negi 7/20/2017 3:46 PM

**Deleted:** c...c21e-f.... Most elevated le... [73]

林田佐智子 7/22/2017 3:00 PM

**Deleted:** season ... [74]

Naveen Negi 7/20/2017 10:22 AM

**Deleted:** connection ...link is not valid ... [74]

Naveen Negi 7/31/2017 4:21 PM

**Deleted:** Most elevated levels of  $XCH_4$  ... [75]

Naveen Negi 6/22/2017 11:50 AM

**Formatted:** Subscript ... [76]

林田佐智子 6/21/2017 5:05 PM

**Deleted:** For example, the emissions fl... [76]

Naveen Negi 8/14/2017 1:14 PM

**Deleted:** ... [77]

Naveen Negi 8/14/2017 1:14 PM

**Deleted:** To study the seasonal  $XCH_4$  p... [77]

Naveen Negi 7/31/2017 4:26 PM

**Deleted:** As shown in Table S1, both tr... [78]

### 3.2 Seasonal cycle of XCH<sub>4</sub> and possible controlling factors

As mentioned earlier, that the persistent deep convection and mean circulation during the SW monsoon season significantly enhance CH<sub>4</sub> in the upper troposphere (e.g., Xiong et al., 2009, Baker et al., 2012), coinciding with the period of high surface CH<sub>4</sub> emissions due to rice paddy cultivation and wetlands over the Indian region (Yan et al., 2009; Hayashida et al., 2013). Although both these emissions and transport processes contribute greatly to seasonal changes in XCH<sub>4</sub>, their relative contributions have not been studied over the monsoon dominated Indian region.

For understanding the role of transport, the atmospheric column is segregated into five sigma-pressure ( $\sigma_p$ ) layers, starting from the surface level ( $\sigma_p = 1$ ) to top of the atmosphere ( $\sigma_p = 0$ ), with an equal layer thickness of  $\sigma_p = 0.2$ . Lower Troposphere (LT), Mid-Troposphere1 (MT1), Mid-Troposphere2 (MT2), Upper Troposphere (UT) and Upper Atmosphere (UA) denote the layers corresponding to the sigma pressure values of 1.0-0.8, 0.8-0.6, 0.6-0.4, 0.4-0.2, and 0.2-0.0. The partial columnar CH<sub>4</sub> are calculated within different  $\sigma_p$  layers (denoted by X<sub>p</sub>CH<sub>4</sub>) using the same formula for XCH<sub>4</sub>, as in Section 2.2. The model results are averaged over each sub-region of our analysis for XCH<sub>4</sub> seasonal cycle. For understanding the role of surface emission in the XCH<sub>4</sub> seasonal cycle, the climatology of optimized total CH<sub>4</sub> flux for each sub-region are compared. Figure 3 shows the monthly mean climatology (average for 2011-2014) of total CH<sub>4</sub> flux, XCH<sub>4</sub> and X<sub>p</sub>CH<sub>4</sub> from the model averaged over three selected regions, EIGP (a1-a7), SP (b1-b7) and AI (c1-c7). These representative regions have been selected because they show distinct XCH<sub>4</sub> seasonal cycles and the dominant controlling factors (such as emission, transport, and chemistry). The observed GOSAT XCH<sub>4</sub> values are also shown for a reference, because the model results do not correspond to the location and time of GOSAT observations (as opposed to those in Figure 2). The plots for the remaining seven regions are available in the supplementary Figures S2 and S3.

Over the EIGP region, magnitude and timing of the seasonal peak in emission differ substantially between the CTL and AGS emission scenarios (ref. Figure 3a7). ACTM simulated XCH<sub>4</sub> seasonal peak is in agreement with the peak in emission in June for AGS case (Figure 3a6). However, simulated XCH<sub>4</sub> remains nearly constant until September, although the emission decreases substantially toward winter. In general, the emission is relatively higher in monsoon season (July-August-September) than in other seasons in both cases. However, in the LT, where we expect most susceptible to the surface emission, the partial column CH<sub>4</sub> indicates very different seasonality from the emissions; X<sub>p</sub>CH<sub>4</sub> (LT) increases toward winter continuously (Figure 3a5). The partial CH<sub>4</sub> columns for the upper troposphere and middle troposphere (Figure 3a2-a3) show similar seasonality to the total XCH<sub>4</sub> rather than in the LT. Therefore, this analysis strongly suggests that the emissions from surface and the upper tropospheric partial column, both contribute to the formation of XCH<sub>4</sub> seasonal cycle. These results also suggest the possibility that GOSAT and ACTM XCH<sub>4</sub> data can be used for correcting a priori emission scenarios by inverse modelling.

In contrast to the XCH<sub>4</sub> seasonal cycle over EIGP, a notable difference is observed in the emission and XCH<sub>4</sub> seasonal cycle over the SP region (Fig. 2b). The XCH<sub>4</sub> seasonal cycle and emission seasonal cycle are found to be out of phase with each other and the differences in emission scenarios are not reflected in XCH<sub>4</sub> seasonal variations. Both emission scenarios show the distinct seasonal pattern; AGS shows annual high emissions from April to September, while CTL shows annual high during August-September (Figure 3b7). The total emissions over SP are much lower than that of EIGP (note the different y-axis scale for Figure 3b7) and hence the difference between the XCH<sub>4</sub> simulations from both emission scenarios is comparatively low. The XCH<sub>4</sub> shows almost identical seasonal cycles for both of the emission scenarios, a peak in October and prolonged low values during

Naveen Negi 7/3/2017 11:49 AM

**Deleted:** As mentioned in introduction earlier, it is well-recognized that the persistent deep convection during the monsoon season uplift the CH<sub>4</sub>-laden air mass from surface to the upper troposphere (Xiong et al., 2009, Baker et al., 2012). However, relative roles of convection and other transport processes, such as the mean circulation or advection, has not been studied. In this section, we discuss the average (2011-2014) XCH<sub>4</sub> annual cycle measured by GOSAT over the study regions discussed in Figure 2. The ACTM simulations with varying surface emissions optimized by the global inverse analysis (Patra et al., 2016), are further used to elucidate the seasonal variation in XCH<sub>4</sub>. To investigate the role contribution of vertical atmospheric layers in to the seasonal XCH<sub>4</sub> cycle., Here the atmospheric column is segregated into five layers according to [79]

林田佐智子 6/21/2017 6:58 PM

**Formatted:** Subscript

林田佐智子 6/21/2017 7:15 PM

**Deleted:** Further, the X<sub>p</sub>CH<sub>4</sub> seasonal cycle in the LT region is only partly vaguely sin [80]

Naveen Negi 8/14/2017 1:11 AM

**Deleted:** -

林田佐智子 6/21/2017 5:40 PM

**Formatted:** Subscript

林田佐智子 6/21/2017 6:51 PM

**Formatted:** Subscript

林田佐智子 6/21/2017 7:14 PM

**Formatted:** Subscript

林田佐智子 6/21/2017 6:57 PM

**Formatted:** Subscript

林田佐智子 6/21/2017 7:00 PM

**Formatted:** Subscript

林田佐智子 6/21/2017 7:11 PM

**Formatted:** Subscript

林田佐智子 6/21/2017 7:14 PM

**Formatted:** Font color: Black

Naveen Negi 7/3/2017 11:56 AM

**Deleted:** seasonal cycle

Naveen Negi 7/31/2017 4:26 PM

**Deleted:** h-n

Prabir Patra 6/19/2017 3:12 PM

**Deleted:** observed incompatible

Prabir Patra 6/19/2017 3:12 PM

**Deleted:** to

林田佐智子 6/21/2017 7:18 PM

**Deleted:** s

Naveen Negi 7/31/2017 4:27 PM

**Deleted:** n

Naveen Negi 7/20/2017 3:54 PM

**Deleted:** n



May to September. The seasonal  $X_p\text{CH}_4$  cycle in the LT layer shows the seasonal pattern similar to the total  $\text{XCH}_4$ . Inconsistency between emission seasonality and  $\text{XCH}_4$  coupled with low emissions strongly suggests that the  $\text{XCH}_4$  can be controlled by transport and/or chemistry, but not emissions. Surface winds during May - September over SP are of the marine origin, which effectively flushes the air with low  $\text{CH}_4$  (see Figure S4). Further, the distinct seasonal cycle of chemical loss is observed over the SP region compared to other study regions; the loss rate starts increasing from 6 ppb  $\text{day}^{-1}$  in January to 12 ppb  $\text{day}^{-1}$  in April, and continue to remain high until September (ref. Figure S5). These pieces of evidence clearly suggest that the combined effect of transport and chemistry causes the low  $\text{XCH}_4$  values for the May-September period over the SP region. The peaks in the upper layers in October (Figure 3b1-b4) and transport from the polluted continental layer in the LT layer (ref. Figure S4) could together contribute to the seasonal  $\text{XCH}_4$  peak over SP. Based on these findings, we conclude that the  $\text{XCH}_4$  measurements do not impose a strong constraint on surface emissions for inverse modelling over the SP region, suggesting a need for in situ measurements.

Over the Arid India (AI) region,  $\text{XCH}_4$  seasonal cycle is observed to be different from those of the EIGP and SI regions. The simulated  $\text{XCH}_4$  (Figure 3c6) show extremely weak sensitivity to the surface emission differences between the AGS and CTL cases (Figure 3c7). Additionally, the  $X_p\text{CH}_4$  in the LT layer (Figure 3c5), does not resemble with the phase of seasonality in surface emissions and simulated/observed  $\text{XCH}_4$ . The  $X_p\text{CH}_4$  in the LT layer decreases from Jan to August and increases until December. On the other hand, a remarkable peak (~1896 ppb) is observed in  $\text{XCH}_4$  during August followed by a decline afterward (Figure 3c6). This is an outstanding example of deceiving linkage between surface emissions and  $\text{XCH}_4$  in terms of seasonal variation. An enhancement in the mixing ratios of  $X_p\text{CH}_4$  is observed from May to August only in the MT2 and UT layers (Figure 3c2-c3) and from June to August in the UA layer (Figure 3c1). This analysis infers that MT2 and UT partial columns mostly contribute in the formation of  $\text{XCH}_4$  seasonal cycle over the AI region.

Next, we quantify the contributions of different partial layers ( $X_p\text{CH}_4$ ) in the formation of  $\text{XCH}_4$  seasonal amplitude (Figure 4). As the phase of  $X_p\text{CH}_4$  seasonal cycle does not always match with that of  $\text{XCH}_4$ , we have fixed months of peak and trough in  $\text{XCH}_4$  seasonal cycle for this analysis. First, we calculate the differences of the  $X_p\text{CH}_4$  values at the time of the peak and the trough of the  $\text{XCH}_4$  over each region, and then the differences at different partial layers are divided by seasonal amplitude of  $\text{XCH}_4$  for calculating the contributions from respective layers into the seasonal amplitude of  $\text{XCH}_4$ .

Figure 4 reveals that ~40% of the seasonal enhancement in the observed  $\text{XCH}_4$  can be attributed to the partial pressure layers below 600 hPa (LT and MT1) for EIGP region, which is directly influenced by the surface emissions. About 40% in seasonal enhancement comes from layers above 600 hPa. Over the SP region, about 60% of the seasonal  $\text{XCH}_4$  amplitude is attributed to layers below 600 hPa and remaining 40% results from the upper layers. Although the activities in the lower atmosphere (below 600 hPa) govern most of the seasonal  $\text{XCH}_4$  cycle over this region, there is no clear link with seasonal variations in emissions as this region is under greater influence of changes in monsoon meteorology. These regions are under the influence of emission signals from the Indian subcontinent during winter; while in the summer, clean marine air control  $\text{CH}_4$  levels (see also Patra et al., 2009). In contrast to the two regions mentioned above, over the AI region, the LT and MT1 layers together contribute only about 12% to the formation of  $\text{XCH}_4$  seasonal cycle amplitude, and the layers above 600 hPa contribute to the remaining 88%. These findings lead us to conclude that instead of surface emissions, the high  $\text{CH}_4$  in the upper tropospheric layers contribute significantly to the formation of seasonal peaks in  $\text{XCH}_4$ .

Naveen Negi 7/31/2017 4:28 PM

**Deleted:** It should be noted that the absolute amount of total emissions are much lower than that of EIGP (note the different y-axis scale of emissions in Figure 3n). On the other hand, being simulated from distinct emissions scenarios having different seasonal cycles, the  $\text{XCH}_4$  shows almost identical seasonal cycles corresponding to for both emission scenarios; a peak in October and broader prolonged low values from during May to September. This suggests that the seasonal cycle of  $\text{XCH}_4$  neither follow the emission pattern, nor the timing of the emission peak over SP. The seasonal  $X_p\text{CH}_4$  cycle in the LT layer over SP shows seasonal pattern similar to the total  $\text{XCH}_4$ , except the peak shifts from October to November. Inconsistency between emission seasonality and  $\text{XCH}_4$  coupled with low emissions strongly suggests that the  $\text{XCH}_4$  can be controlled by transportation and/or chemistry, not emission

林田佐智子 6/21/2017 7:26 PM

Formatted: Subscript

林田佐智子 6/21/2017 7:26 PM

Formatted: Subscript

Naveen Negi 8/14/2017 1:22 PM

**Deleted:** Surface winds from May to September over SP are from the southern hemisphere, which effectively flushes the air with low  $\text{CH}_4$  and pushes the polluted air masses from the south to the north India region (refer to supplementary Figure S4). Further, the distinct seasonal cycle of chemical loss is observed over the SP region (refer to supplementary Figure S5) compared to other study regions; the loss rate starts increasing from 6 ppb  $\text{day}^{-1}$  in January to 12 ppb  $\text{day}^{-1}$  in April. [81]

Prabir Patra 6/19/2017 3:34 PM

Moved (insertion) [4]

Naveen Negi 7/3/2017 12:02 PM

**Deleted:** Over the Arid India (AI) region, the seasonal  $\text{XCH}_4$  cycle is different from those of the EIGP and SI regions. At a first glance, it seems the  $\text{XCH}_4$  simulations (Figure 3t) ... [82]

Prabir Patra 6/19/2017 3:27 PM

Formatted: Highlight

Prabir Patra 6/19/2017 3:34 PM

**Moved down [4]:** In contrast to previous two regions, EIGP and SI, over the AI region, the seasonal  $\text{XCH}_4$  variation in the LT and MT1 layers together contribute only about 12% ... [83]

Prabir Patra 6/19/2017 3:25 PM

**Moved down [3]:** Similarly, Figure 4, Figure S2 and Figure S3 indicate that more than 60% in the seasonal amplitude of  $\text{XCH}_4$  comes below 600 hPa over the regions lying in ... [84]

Prabir Patra 6/19/2017 3:25 PM

Moved (insertion) [3]

### 3.3 Source of higher CH<sub>4</sub> in the upper troposphere

The reason of high mixing ratios in the upper troposphere, as discussed in the former section, can be explained by vertical transport of high CH<sub>4</sub> emission signal from the surface, because the vertical transport time scales in the tropical region is much shorter than chemical lifetime of CH<sub>4</sub> of the order of 1-2 years (Patra et al., 2009). Figure 5a1-a4 shows the latitude-pressure cross-sections of the convective transport rate (in ppb day<sup>-1</sup>) and vertical velocity (hPa s<sup>-1</sup>) averaged over 83-93°E for different seasons of 2011 (the ACTM AGS case). The positive/negative values of convective transport rate and vertical velocity in Figure 5a1-a4 indicate the gain/loss of mass and downward/upward motions, respectively. Rapid updrafts of CH<sub>4</sub>, as indicated by higher negative vertical velocity, by deep convection during the monsoon season are aided by the regional topography of the IGP region (north of 20°N and east of 79°E in the Indian region). These updrafts lift CH<sub>4</sub>-rich air into the upper tropospheric region (Figure 5b3). The CH<sub>4</sub> concentrations at the surface level decreased rapidly at an average rate of ~10 ppb day<sup>-1</sup> during the SW monsoon season, and accumulate in the upper troposphere at a similar rate over IGP region (Figure 5a3). During the winter, spring and autumn season surface CH<sub>4</sub> decreased at an average rate of 2 ppb day<sup>-1</sup>, 8 ppb day<sup>-1</sup> and 7 ppb day<sup>-1</sup>, respectively. CH<sub>4</sub> levels accumulate in the middle and upper troposphere at an average rate of 6 ppb day<sup>-1</sup> during the spring and autumn season while during winter season no significant accumulation has been observed at this height over IGP region (Figure 5a1, a2, a4). Overall these transport processes repeat every year with a certain degree of interannual variations as can be seen for the years from 2011 to 2014. The interannual variations are likely to have been caused by the early/late onset and retreat of the SW monsoon as well as the weak/strong monsoon activity over the years.

The horizontal cross-sections of CH<sub>4</sub> at 200 hPa are shown with wind vectors in Figure 5c1-c4 for understanding the spatial extent of uplifted CH<sub>4</sub>-rich air over the whole South Asian region. The uplifted CH<sub>4</sub>-rich air mass is trapped in the upper troposphere (~200 hPa), when encountered by the anticyclonic winds during the SW monsoon season. This leads to a widespread CH<sub>4</sub> enhancement covering the large part of South Asia, and the CH<sub>4</sub>-rich air leaked predominantly along the southern side of the sub-tropical westerly jet over to the East Asia (Figure 5c3; see also Umezawa et al., 2012). As a result of this, the high CH<sub>4</sub> air masses at upper troposphere are not limited to the regions of intense surface emissions as discussed earlier. After the SW monsoon season, the strong westerly jet breaks the upper tropospheric anticyclone and the CH<sub>4</sub>-rich air mass shifts over southern India during the autumn season (Figure 5c4). In this way, the convective updraft of high-CH<sub>4</sub> air mass, followed by horizontal spreading of the air mass over the larger area by anticyclonic circulation, controls the redistribution of CH<sub>4</sub> in the upper troposphere over the northern part of India during SW monsoon season, and over southern peninsula during the early autumn season.

### 4. Conclusions

The seasonal variations in dry-air mole fractions of methane (XCH<sub>4</sub>) measured by GHGs Observation SATellite (GOSAT) are analyzed over India and the surrounding seas using the JAMSTEC's atmospheric chemistry-transport model (ACTM). The region of interest (Indian landmass) is divided into 8 sub-regions, namely, Northeast India (NEI), Eastern India (EI), Eastern IGP (EIGP), Western IGP (WIGP), Central India (CI), Arid India (AI), Western India (WI), Southern Peninsula (SP), and two surrounding oceanic regions, the Arabian Sea (AS) and Bay of Bengal (BOB). The ACTM simulations are conducted using a couple of surface fluxes optimized by the inverse analysis as described in Patra et al. (2016). We have shown that the distinct spatial and temporal variations of XCH<sub>4</sub> observed by GOSAT are not only governed by the heterogeneity in surface emissions,

Naveen Negi 8/14/2017 1:09 AM

**Deleted:** Using ACTM simulations, we have shown that the higher CH<sub>4</sub> levels in the upper tropospheric region (~400-200 hPa) during the monsoon season contribute significantly to enhanced XCH<sub>4</sub> values over the northern regions of India regions. The source of higher mixing ratios in the upper troposphere as discussed in previous section can be explained by vertical transport of the CH<sub>4</sub> emitted emission signal from the surface, because the vertical transport timescales in the tropical region no is much shorter than chemical lifetime of CH<sub>4</sub> of the order of 1-2 years source is present at this height (Patra et al., 2009). Figure 5a-d shows the latitudinal cross section of the convective transport rate (in ppb day<sup>-1</sup>) along with height and vertical velocity [85]

林田佐智子 6/21/2017 7:46 PM

**Formatted:** Subscript

Prabir Patra 6/19/2017 3:50 PM

**Deleted:** Like in Section 3.2, previous studies also show a shift in XCH<sub>4</sub> seasonal peak [86]

Naveen Negi 6/23/2017 11:06 AM

**Formatted:** Plain Text, Justified, Line spacing: 1.5 lines

Prabir Patra 6/19/2017 3:59 PM

**Deleted:** were closely

Prabir Patra 6/19/2017 3:59 PM

**Deleted:** here

Naveen Negi 7/3/2017 12:19 PM

**Deleted:**

Naveen Negi 7/31/2017 4:34 PM

**Deleted:**

Prabir Patra 6/19/2017 4:00 PM

**Deleted:** JAMSTEC's atmospheric chemistry-transport model (

Prabir Patra 6/19/2017 4:00 PM

**Deleted:** ) of CH<sub>4</sub> and

Naveen Negi 7/3/2017 12:19 PM

**Deleted:** total

Prabir Patra 6/19/2017 4:01 PM

**Deleted:** are used for bridging the transport and emission information to observed X [87]

Naveen Negi 7/3/2017 12:20 PM

**Deleted:** for two a priori scenarios.

Prabir Patra 6/19/2017 4:02 PM

**Deleted:** have been observed

Prabir Patra 6/19/2017 4:02 PM

**Deleted:** that

Prabir Patra 6/19/2017 4:02 PM

**Deleted:** features

Prabir Patra 6/19/2017 4:02 PM

**Deleted:** ous

Naveen Negi 7/31/2017 4:34 PM

**Deleted:** ,

but also due to complex atmospheric transport mechanisms caused by the seasonally varying Asian monsoon. The seasonal XCH<sub>4</sub> patterns often show a fair correlation between emissions and XCH<sub>4</sub> over the regions residing in the northern half of India (north of 15°N: NEI, EI, EIGP, WIGP, CI, WI, AI), which would imply XCH<sub>4</sub> levels are closely associated with the distribution of emissions on the Earth's surface. However, detailed analysis of transport and emission using ACTM over these regions (except for the AI) reveal that about 40% of seasonal enhancement in the observed XCH<sub>4</sub> can be attributed to the lower tropospheric layer (below 600 hPa). The lower tropospheric layer are either affected by the surface emissions, e.g., in the northern India regions or seasonal changes in horizontal winds due to monsoon for the SP. Up to 40% of the seasonal CH<sub>4</sub> enhancement is found to come from the uplifted air mass in to the 600-200 hPa height layer over northern regions in India. In contrast, over semi-arid AI region, as much as ~88% contributions to the XCH<sub>4</sub> seasonal cycle amplitude came from the height above 600 hPa, and only ~12% are contributed by the atmosphere below 600 hPa. The primary cause of the higher contributions from above 600 hPa over the northern Indian region is the characteristic of air mass transport mechanisms in the Asian monsoon region. The persistent deep convection during the southwest monsoon season (June-August) causes strong updrafts of CH<sub>4</sub>-rich air mass from the surface to upper tropospheric heights (~200 hPa), which is then confined by anticyclonic winds at this height. The anticyclonic confinement of surface emission over a wider South Asia region leads to strong contribution of the upper troposphere in formation of the XCH<sub>4</sub> peak over most regions in northern India, including the semi-arid regions with extremely low CH<sub>4</sub> emissions. In contrast to these regions, over the SP region, the major contributions (about 60%) to XCH<sub>4</sub> seasonal amplitude come from the lower atmosphere (~1000-600 hPa). Both transport and chemistry dominate in the lower troposphere over SP region and thus the formation of XCH<sub>4</sub> seasonal cycle is not consistent with the seasonal cycle of local emissions. As the upper level anticyclone does not cover the southern Indian region during the active phase of southwest monsoon, no enhancement in XCH<sub>4</sub> is observed over the southern peninsular region.

This study shows that ACTM simulations are well capturing the GOSAT observed seasonal and spatial XCH<sub>4</sub> variability and points to a comprehensive understanding of emissions, chemistry, and transport of CH<sub>4</sub> over one of the strongest global monsoonal regions. This provides extremely important for perceptive insights into the source-receptor relationships. Our results provide strong support for performing inverse modelling of CH<sub>4</sub> surface emissions in the future using XCH<sub>4</sub> observations and ACTM forward simulation.

#### Acknowledgements

The Environment Research and Technology Development Fund (A2-1502) of the Ministry of the Environment, Japan, supported this research. The data used for preparing the figures, and table could be available on request. The corresponding author may be contacted for the same.

#### References

- Baker, A. K., Schuck, T. J., Brenninkmeijer, C. A. M., Rauthe-Schöch, A., Slemr, F., van Velthoven, P. F. J., and Lelieveld, J.: Estimating the contribution of monsoon-related biogenic production to methane emissions from South Asia using CARIBIC observations, *Geophys. Res. Lett.*, 39, L10813, doi:10.1029/2012GL051756, 2012.
- Crutzen, P.J., Aselmann, I., and Seiler, W.: Methane production by domestic animals, wild ruminants other herbivorous fauna and humans. *Tellus* 38B, 271-284, doi:10.1111/j.1600-0889.1986.tb00193.x, 1986.

Prabir Patra 6/19/2017 4:04 PM

Deleted: ies

Prabir Patra 6/19/2017 4:04 PM

Deleted: sources

Naveen Negi 7/3/2017 12:21 PM

Deleted: . However, detailed analysis of transport and emission using ACTM reveal that only less than 40% of seasonal enhancement in the observed XCH<sub>4</sub> can be attributed to surface emissions over these regions except AI, as only this amount of CH<sub>4</sub> enhancement is available in the lower troposphere (below 600 hPa), which is directly affected by the surface emissions. In fact,

Prabir Patra 6/19/2017 4:06 PM

Deleted: ~

Naveen Negi 7/3/2017 12:21 PM

Deleted: -60

Prabir Patra 6/19/2017 4:07 PM

Deleted: in

Prabir Patra 6/19/2017 4:07 PM

Deleted: between

Naveen Negi 7/3/2017 12:22 PM

Deleted: these regions

Naveen Negi 8/14/2017 1:47 PM

Deleted: o

Prabir Patra 6/19/2017 4:08 PM

Deleted: ation

Prabir Patra 6/19/2017 4:08 PM

Deleted: s

Naveen Negi 7/31/2017 4:35 PM

Deleted: The persistent deep convection during the southwest (SW) monsoon season (June-August) causes strong updrafts of CH<sub>4</sub> from the surface to upper troposphere, which is then distributed by anticyclonic winds over the northern Indian region. These transport mechanisms caused the elevated CH<sub>4</sub> mixing ratios in the upper troposphere hence contributed significantly to the seasonal peak in XCH<sub>4</sub> over northern India. In contrast to these regions, over the Southern Peninsular region, the major contributions (about 60%) to XCH<sub>4</sub> seasonal amplitude come from the lower atmosphere (~1000-600 hPa). Both transport and chemistry dominate in the lower atmosphere over SP region and thus, as a result of it, the seasonal variation of XCH<sub>4</sub> is do not corresponding to the seasonality of the local emissions. As the upper level anticycl...

Naveen Negi 7/3/2017 12:23 PM

Deleted: s that s are generally the s to emissions, chemistry and Our results provide strong support foring .

Prabir Patra 6/19/2017 4:01 PM

Deleted: Most satellite sensors are designed to provide total column observations of atmospheric chemical species. This stu...

- 572 Cao, M., Gregson, K., and Marshall, S.: Global methane emission from wetlands and its sensitivity to climate change. *Atmos.*  
573 *Environ.* 32 (19), 3293-3299, doi:10.1016/S1352-2310 (98) 00105-8, 1998.
- 574 Chandra, N., Venkataramani, S., Lal, S., Sheel, V. & Pozzer, A.: Effects of convection and long-range transport on the  
575 distribution of carbon monoxide in the troposphere over India. *Atmospheric Pollution Research* 7, 775 – 785,  
576 doi:10.1016/j.apr.2016.03.005, 2016.
- 577 Dlugokencky, E. J., Nisbet, E. G., Fisher, R., and Lowry, D.: Global atmospheric methane: Budget, changes, and dangers, *Philos.*  
578 *Trans. R. Soc. London, Ser. A.*, 369, 2058–2072, 2011.
- 579 EDGAR42FT, 2013: Global emissions EDGAR v4.2FT2010 (October 2013). [Available at  
580 <http://edgar.jrc.ec.europa.eu/overview.php?v=42FT2010>.]
- 581 Fung, I., John, J., Lerner, J., Matthews, E., Prather, M., Steele, L. P., and Fraser, P. J.: Three-dimensional model synthesis of the  
582 global methane cycle, *J. Geophys. Res.*, 96, 13033–13065, doi:10.1029/91JD01247, 1991
- 583 [Frankenberg, C., P. Bergamaschi, A. Butz, S. Houweling, J. F. Meirink, J. Notholt, A. K. Petersen, H. Schrijver, T. Warneke,](#)  
584 [and I. Aben \(2008\), Tropical methane emissions: A revised view from SCIAMACHY onboard ENVISAT, \*Geophys. Res. Lett.\*, 35\(15\), doi:10.1029/2008gl034300.](#)
- 586 [Frankenberg, C., I. Aben, P. Bergamaschi, E. J. Dlugokencky, R. van Hees, S. Houweling, P. van der Meer, R. Snel, and P. Tol](#)  
587 [\(2011\), Global column-averaged methane mixing ratios from 2003 to 2009 as derived from SCIAMACHY: Trends and](#)  
588 [variability, \*J. Geophys. Res.\*, 116\(D4\), doi:10.1029/2010jd014849.](#)
- 589 [Gillett N. P., and H. D. Matthews \(2010\), Accounting For Carbon Cycle Feedbacks in a Comparison of the Global Warming](#)  
590 [Effects of Greenhouse Gases, \*Environ. Res. Lett.\* 5, 034011 \(2010\).](#)
- 591 [Hayashida, S., Ono, A., Yoshizaki, S., Frankenberg, C., Takeuchi, W., Yan, X.: Methane concentrations over Monsoon Asia as](#)  
592 [observed by SCIAMACHY: Signals of methane emission from rice cultivation. \*Remote Sensing of Environment\* 139, 246–](#)  
593 [256, doi: 10.1016/j.rse.2013.08.008, 2013.](#)
- 594 Kuze, A., Suto, H., Nakajima, M., and Hamazaki, T.: Thermal and near infrared sensor for carbon observation Fourier transform  
595 spectrometer on the Greenhouse Gases Observing Satellite for greenhouse gases monitoring. *Appl. Opt.* 48, 6716–6733, doi:  
596 10.1364/AO.48.006716, 2009.
- 597 Kar, J., Deeter, M. N., Fishman, J., Liu, Z., Omar, A., Creilson, J. K., Treppe, C. R., Vaughan, M. A., and Winker, D. M.:  
598 Wintertime pollution over the Eastern Indo-Gangetic Plains as observed from MOPITT, CALIPSO and tropospheric ozone  
599 residual data, *Atmos. Chem. Phys.*, 10, 12273-12283, doi:10.5194/acp-10-12273-2010, 2010.
- 600 Kavitha, M. and Nair, P. R.: Region-dependent seasonal pattern of methane over Indian region as observed by SCIAMACHY.  
601 *Atmospheric Environment* 131, 316–325, doi:10.1016/j.atmosenv.2016.02.008, 2016.
- 602 Lal, S., Venkataramani, S., Chandra, N., Cooper, O. R., Brioude, J., and Naja, M.: Transport effects on the vertical distribution of  
603 tropospheric ozone over western India, *J. Geophys. Res. Atmos.*, 119, 10,012–10,026, doi:10.1002/2014JD021854, 2014.
- 604 [Matthews, E., and Fung, I.: Methane emissions from natural wetlands: Global distribution, area and environmental](#)  
605 [characteristics of sources. \*Global Biogeochem. Cycles\* 1, 61-86, 1987.](#)
- 606 Minami, K., and Neue, H. U.: Rice paddies as a methane source. *Clim. Change Lett.* 27, 13-26, doi:10.1007/BF01098470, 1994.
- 607 Morino, I., Uchino, O., Inoue, M., Yoshida, Y., Yokota, T., Wennberg, P. O., Toon, G. C., Wunch, D., Roehl, C. M., Notholt, J.,  
608 Warneke, T., Messerschmidt, J., Griffith, D. W. T., Deutscher, N. M., Sherlock, V., Connor, B., Robinson, J., Sussmann, R.,  
609 and Rettinger, M.: Preliminary validation of column-average volume mixing ratios of carbon dioxide and methane retrieved  
610 from GOSAT short-wavelength infrared spectra. *Atmos. Meas. Tech.*, 4, 1061–1076, doi:10.5194/amt-4-1061-2011, 2011.

林田佐智子 6/21/2017 4:24 PM

Formatted: Font:10 pt

林田佐智子 6/21/2017 4:25 PM

Formatted: Indent: Left: 0", Hanging: 2 ch, First line: -2 ch, Line spacing: 1.5 lines

Naveen Negi 8/14/2017 1:08 AM

Formatted: Indent: Left: 0", Hanging: 2 ch, First line: -2 ch, Line spacing: 1.5

Naveen Negi 8/14/2017 1:08 AM

Formatted: Font:10 pt

林田佐智子 6/21/2017 4:20 PM

Deleted: Frankenberg, C., Meirink, J. F., van Weele, M., Platt, U., and Wagner, T.: Assessing methane emissions from global space-borne observations, *Science*, 308, 1010–1014, 2005. .

91



- 517 Myhre, G., Shindell, D., Bréon, F.-M., Collins, W. Fuglested, J., Huang, J., Koch, D. Lamarque, J.-F., Lee, D., Mendoza, B.,  
 518 Nakajima, T., Robock, A., Stephens, G. Takemura, T., and Zhang, H.: Anthropogenic and natural radiative forcing, in:  
 519 Climate Change 2013: The Physical Science Basis, Fifth Assessment Report of the Intergovernmental Panel on Climate  
 520 Change, edited by: Stocker, T. F. et al., Cambridge University Press, Cambridge, UK, New York, NY, USA, 659–740, 2013.
- 521 Olivier, J. G. J., Aardenne, J.A.V., Dentener, F., Ganzeveld, L. N., Peters, J.A.H.W.: Recent trends in global greenhouse gas  
 522 emissions: Regional trends and spatial distribution of key sources, in: Non-CO<sub>2</sub> Greenhouse Gases (NCGG-4), edited by:  
 523 van Amstel, A., 325–330, Millpress, Rotterdam, Netherlands, 2005.
- 524 Onogi, K., Tsutsui, J., Koide, H., Sakamoto, M., Kobayashi, S., Hatsushika, H. Matsumoto, T., Yamazaki, N., Kamahori, H.,  
 525 Takahashi, K., Kadokura, S., Wada, K., Kato, K., Oyama, R., Ose, T., Mannoji, N., and Taira, R.: The JRA-25 reanalysis, *J.*  
 526 *Meteorol. Soc. Jpn.*, 85, 369–432, 2007.
- 527 Park, M., Randel, W. J., Kinnison, D. E., Garcia, R. R., and Choi, W.: Seasonal variation of methane, water vapor, and nitrogen  
 528 oxides near the tropopause: Satellite observations and model simulations. *Journal of Geophysical Research: Atmospheres*  
 529 109, doi: 10.1029/2003JD003706. D03302, 2004.
- 530 Patra, P. K., Takigawa, M., Ishijima, K., Choi, B. C., Cunnold, D., Dlugokencky, E. J., Fraser, P., A. J., Gomez-Pelaez, Goo, T.  
 531 Y., Kim, J. S., Krummel, P., Langenfelds, R., Meinhardt, F., Mukai, H., O'Doherty, S., Prinn, R. G., Simmonds, P., Steele,  
 532 P., Tohjima, Y., Tsuboi, K., Uhse, K., Weiss, R., Worthy, D., and Nakazawa, T.: Growth rate, seasonal, synoptic, diurnal  
 533 variations and budget of methane in lower atmosphere, *J. Meteorol. Soc. Jpn.*, 87(4), 635–663, doi: 10.2151/jmsj.87.635,  
 534 2009.
- 535 Patra, P. K., Houweling, S., Krol, M., Bousquet, P., Belikov, D., Bergmann, D., Bian, H., Cameron-Smith, P., Chipperfield, M.  
 536 P., Corbin, K., Fortems-Cheiney, A., Fraser, A., Gloor, E., Hess, P., Ito, A., Kawa, S. R., Law, R. M., Loh, Z., Maksyutov,  
 537 S., Meng, L., Palmer, P. I., Prinn, R. G., Rigby, M., Saito, R., and Wilson, C.: TransCom model simulations of CH<sub>4</sub> and  
 538 related species: Linking transport, surface flux and chemical loss with CH<sub>4</sub> variability in the troposphere and lower  
 539 stratosphere, *Atmos. Chem. Phys.*, 11, 12,813–12,837, doi:10.5194/acp-11-12813-2011, 2011a.
- 540 [Patra, P. K., Niwa, Y., Schuck, T. J., Brenninkmeijer, C. A. M., Machida, T., Matsueda, H., and Sawa, Y.: Carbon balance of](#)  
 541 [South Asia constrained by passenger aircraft CO<sub>2</sub> measurements, \*Atmos. Chem. Phys.\*, 11, 4163–4175. doi:10.5194/acp-11-](#)  
 542 [4163-2011, 2011b.](#)
- 543 [Patra, P. K., Canadell, J. G., Houghton, R. A., Piao, S. L., Oh, N.-H., Ciais, P., Manjunath, K. R., Chhabra, A., Wang, T.,](#)  
 544 [Bhattacharya, T., Bousquet, P., Hartman, J., Ito, A., Mayorga, E., Niwa, Y., Raymond, P. A., Sarma, V. V. S. S., and Lasco,](#)  
 545 [R.: The carbon budget of South Asia, \*Biogeosciences\*, 10, 513–527. doi:10.5194/bg-10-513-2013, 2013.](#)
- 546 Patra, P. K., Krol, M. C., Montzka, S. A., Arnold, T., Atlas, E. L., Lintner, B. R., Stephens, B. B., Xiang, B., Elkins, J. W.,  
 547 Fraser, P. J., Ghosh, A., Hintsa, E. J., Hurst, D. F., Ishijima, K., Krummel, P. B., Miller, B. R., Miyazaki, K., Moore, F. L.,  
 548 Mühle, J., O'Doherty, S., Prinn, R. G., Steele, L. P., Takigawa, M., Wang, H. J., Weiss, R. F., Wofsy, S. C., and Young, D.:  
 549 Observational evidence for interhemispheric hydroxyl parity, *Nature*, 513, 219–223, 2014.
- 550 Patra, P. K., Saeki, T., Dlugokencky, E. J., Ishijima, K., Umezawa, S. T., Ito, A., Aoki, S., Morimoto, S., Kort, E. A., Crotwell, A.,  
 551 Kumar, R., and Nakazawa, T.: Regional methane emission estimation based on observed atmospheric concentrations (2002–  
 552 2012), *J. Meteorol. Soc. Jpn.*, 94(1), 91–113, doi:10.2151/jmsj.2016-006, 2016.
- 553 Rao, Y. P.: Southwest monsoon: Synoptic Meteorology, Meteor. Monogr., No. 1/1976, India Meteorological Department, 367  
 554 pp, 1976.
- 555 Randel, W. J. and Park, M.: Deep convective influence on the Asian summer monsoon anticyclone and associated tracer

Naveen Negi 7/31/2017 4:37 PM

**Deleted:** Olsen, K. S., Strong, K., Walker, K. A., Boone, C. D., Raspollini, P., Plieninger, J., Bader, W., Conway, S., Grutter, M., Hannigan, J. W., Hase, F., Jones, N., de Mazière, M., Notholt, J., Schneider, M., Smale, D., Sussmann, R., and Saitoh, N.: Comparison of the GOSAT TANSO-FTS TIR CH<sub>4</sub> volume mixing ratio vertical profiles with those measured by ACE-FTS, ESA MIPAS, IMK-IAA MIPAS, and 16 NDACC stations, *Atmos. Meas. Tech. Discuss.*, doi:10.5194/amt-2017-6, in review, 2017.

- 569 variability observed with Atmospheric Infrared Sounder (AIRS). *J. Geophys. Res.* 111, doi: 10.1029/2005JD006490, 2006.
- 570 Sugimoto, A., Inoue, T., Kirtibutr, N. and Abe, T.: Methane oxidation by termite mounds estimated by the carbon isotopic  
571 composition of methane. *Glob. Biogeochem. Cycles* 12 (4), 595-605, doi:10.1029/98GB02266, 1998.
- 572 Shindell, D. T., Faluvegi, G., Koch, D. M., Schmidt, G. A., Unger, N., Bauer, S. E.: Improved attribution of climate forcing to  
573 emissions, *Science*, 326, 716-718, doi: 10.1126/science.1174760, 2009.
- 574 Schuck, T. J., Ishijima, K., Patra, P. K., Baker, A. K., Machida, T., Matsueda, H., Sawa, Y., Umezawa, T., Brenninkmeijer, C. A.  
575 M., and Lelieveld, J.: Distribution of methane in the tropical upper troposphere measured by CARIBIC and CONTRAIL  
576 aircraft, *J. Geophys. Res.*, 117, D19304, doi:10.1029/2012JD018199, 2012.
- 577 Spivakovsky, C. M., Logan, J. A., Montzka, S. A., Balkanski, Y. J., Foreman-Fowler, M., Jones, D. B. A., Horowitz, L.  
578 W., Fusco, A. C., Brenninkmeijer, C. A. M., Prather, M. J., Wofsy, S. C., and McElroy, M. B.: Three-dimensional  
579 climatological distribution of tropospheric OH: update and evaluation, *J. Geophys. Res.*, 105, 8931-8980,  
580 doi:10.1029/1999JD901006, 2000.
- 581 [Umezawa, T., Machida, T., Ishijima, K., Matsueda, H., Sawa, Y., Patra, P. K., Aoki, S., and Nakazawa, T. Carbon and hydrogen  
582 isotopic ratios of atmospheric methane in the upper troposphere over the Western Pacific, \*Atmos. Chem. Phys.\*, 12, 8095-  
583 8113, 2012.](#)
- 584 [Wunch, D., G. C. Toon, J.-F. L. Blavier, R. A. Washenfelder, J. Notholt, B. J. Connor, D. W. T. Griffith, V. Sherlock, and P. O.  
585 Wennberg, The total carbon column observing network, \*Phil. Trans. Royal Society - Series A\*, 369, 2087-2112,  
586 doi:10.1098/rsta.2010.0240, 2011.](#)
- 587 Xiong, X., Houweling, S., Wei, J., Maddy, E., Sun, F., and Barnet, C.: Methane plume over south Asia during the monsoon  
588 season: satellite observation and model simulation, *Atmos. Chem. Phys.*, 9, 783-794, doi:10.5194/acp-9-783-2009, 2009.
- 589 [Yoshida, Y., Y. Ota, N. Eguchi, N. Kikuchi, K. Nobuta, H. Tran, I. Morino, and T. Yokota \(2011\), Retrieval algorithm for CO<sub>2</sub>  
590 and CH<sub>4</sub> column abundances from short-wavelength infrared spectral observations by the Greenhouse gases observing  
591 satellite, \*Atmospheric Measurement Techniques\*, 4\(4\), 717-734, doi:10.5194/amt-4-717-2011.](#)
- 592 Yoshida, Y., Kikuchi, N., Morino, I., Uchino, O., Oshchepkov, S., Bril, A., Saeki, T., Schutzgens, N., Toon, G. C., Wunch, D.,  
593 Roehl, C. M., Wennberg, P. O., Griffith, D. W. T., Deutscher, N. M., Warneke, T., Notholt, J., Robinson, J., Sherlock, V.,  
594 Connor, B., Rettinger, M., Sussmann, R., Ahonen, P., Heikkinen, P., Kyrö, E., Mendonca, J., Strong, K., Hase, F., Dohe, S.,  
595 and Yokota, T.: Improvement of the retrieval algorithm for GOSAT SWIRXCO<sub>2</sub> and XCH<sub>4</sub> and their validation using  
596 TCCON data, *Atmos. Meas. Tech.*, 6, 1533-1547, doi:10.5194/amt-6-1533-2013, 2013.
- 597 Yan, X., Akiyama, H., Yagi, K., and Akimoto, H.: Global estimations of the inventory and mitigation potential of methane  
598 emissions from rice cultivation conducted using the 2006 Intergovernmental Panel on Climate Change Guidelines, *Global  
599 Biogeochem. Cycles*, 23, GB2002, doi:10.1029/2008GB003299, 2009.

Naveen Negi 7/31/2017 4:38 PM

**Deleted:** Worden, J. R., Turner, A. J., Bloom, A., Kulawik, S. S., Liu, J., Lee, M., Weidner, R., Bowman, K., Frankenberg, C., Parker, R., and Payne, V. H.: Quantifying lower tropospheric methane concentrations using GOSAT near-IR and TES thermal IR measurements, *Atmos. Meas. Tech.*, 8, 3433-3445, doi:10.5194/amt-8-3433-2015, 2015. .

Naveen Negi 6/22/2017 10:52 AM

**Deleted:** <sub>

Naveen Negi 6/22/2017 10:52 AM

**Deleted:** </sub>

Naveen Negi 6/22/2017 10:52 AM

**Formatted:** Subscript

Naveen Negi 6/22/2017 10:52 AM

**Deleted:** <sub>

Naveen Negi 6/22/2017 10:53 AM

**Formatted:** Subscript

Naveen Negi 6/22/2017 10:52 AM

**Deleted:** </sub>

Naveen Negi 7/31/2017 4:38 PM

**Deleted:** Zou, M., Xiong, X., Saitoh, N., Warner, J., Zhang, Y., Chen, L., Weng, F., and Fan, M.: Satellite observation of atmospheric methane: intercomparison between AIRS and GOSAT TANSO-FTS retrievals, *Atmos. Meas. Tech.*, 9, 3567-3576, doi:10.5194/amt-9-3567-2016, 2016. .

Naveen Negi 8/14/2017 1:04 PM

**Formatted:** Left

Naveen Negi 6/23/2017 12:14 PM

**Deleted:** .

**Figures and Table.**

Table 1: Correlation coefficients (R) between observed and model simulated seasonal cycles of XCH<sub>4</sub>. Model simulations are obtained from ACTM using two different emission scenarios, AGS and CTL. The details of these scenarios are given in Patra et al (2016).

<u>Site/ Tracer</u>	<u>ACTM AGS</u>	<u>ACTM CTL</u>
<u>Arid India</u>	<u>0.77</u>	<u>0.88</u>
<u>WIGP region</u>	<u>0.86</u>	<u>0.90</u>
<u>EIGP region</u>	<u>0.69</u>	<u>0.88</u>
<u>Northeast India</u>	<u>0.55</u>	<u>0.55</u>
<u>Western India</u>	<u>0.87</u>	<u>0.95</u>
<u>Central India</u>	<u>0.89</u>	<u>0.97</u>
<u>East India</u>	<u>0.78</u>	<u>0.86</u>
<u>Southern Peninsula</u>	<u>0.92</u>	<u>0.91</u>
<u>Arabian Sea</u>	<u>0.86</u>	<u>0.87</u>
<u>Bay of Bengal</u>	<u>0.84</u>	<u>0.86</u>

Naveen Negi 6/23/2017 12:14 PM

Deleted: -

[92]

Naveen Negi 6/23/2017 12:14 PM

Formatted: Font:12 pt

Naveen Negi 8/14/2017 1:04 PM

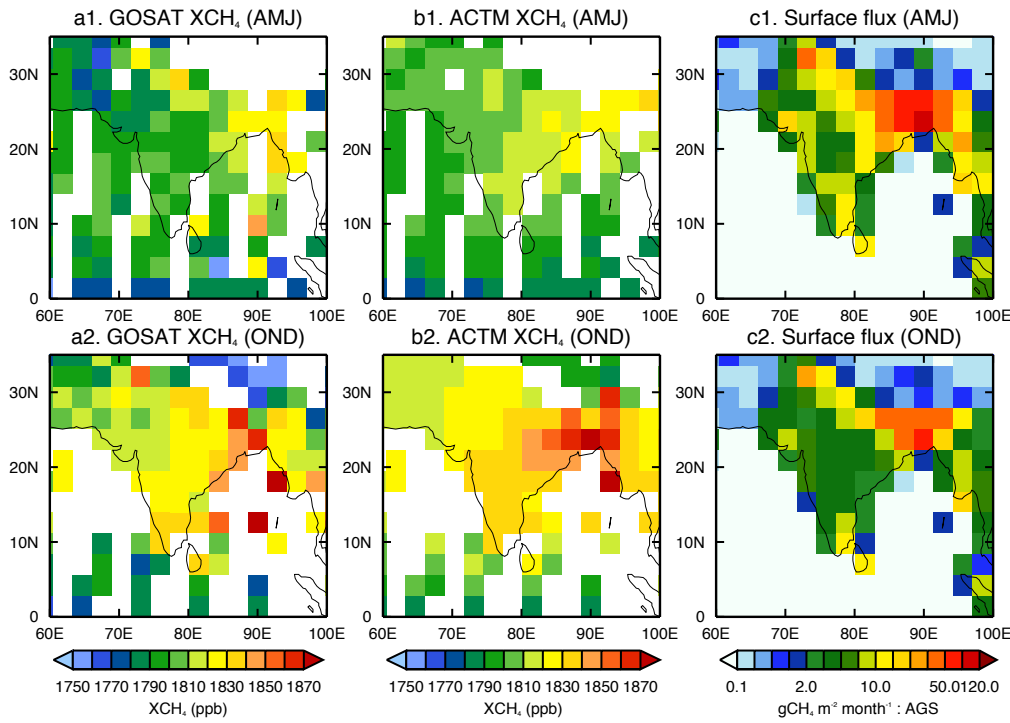
Formatted: Centered

Naveen Negi 6/23/2017 12:14 PM

Formatted: Font:12 pt

Naveen Negi 6/23/2017 12:14 PM

Formatted: Font:12 pt



738  
739  
740  
741  
742  
743  
744  
745

**Figure 1:** Average seasonal distributions (from 2011 to 2014) of XCH<sub>4</sub> obtained from GOSAT observations (a1-a2), ACTM simulations (b1-b2) and CH<sub>4</sub> emission consisting of all the natural and anthropogenic emissions (c1-c2; ACTM\_AGS case) over the Indian region. Optimized emissions are shown from a global inversion of surface CH<sub>4</sub> concentrations (Patra et al., 2016) and multiplied by a constant factor of 12 for a clear visualization. The ACTM is first sampled at the location and time of GOSAT observations and then seasonally averaged. The white spaces in panels (a1-b2) are due to the missing data caused by satellite retrieval limitations from cloud cover.

Naveen Negi 7/31/2017 4:41 PM

Deleted:

Unknown

Formatted: Font:(Default) Times New Roman, 10 pt

---

Naveen Negi 7/31/2017 4:38 PM

Deleted: b

Naveen Negi 7/31/2017 4:39 PM

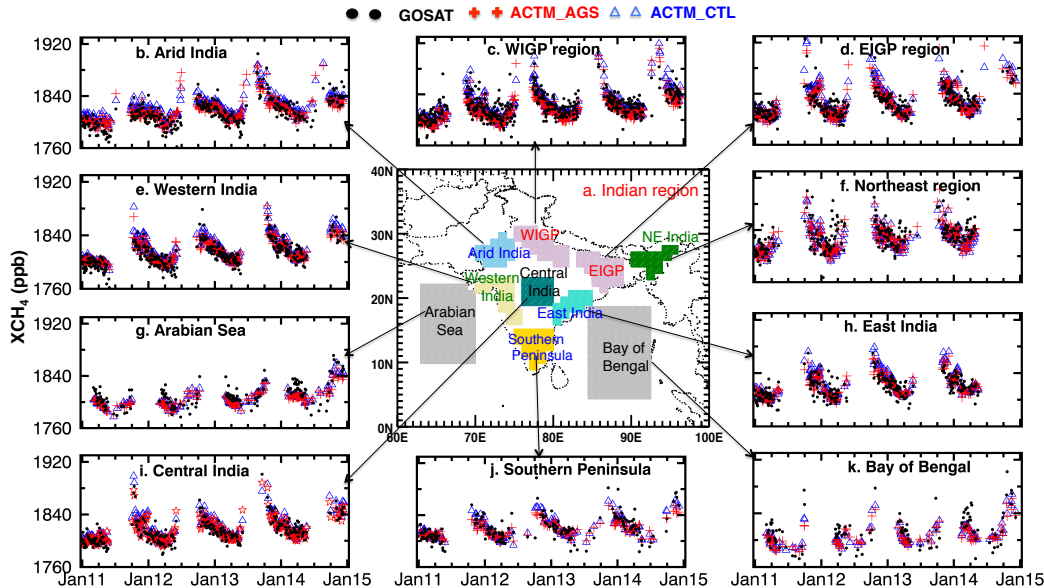
Deleted: c-d

Naveen Negi 7/31/2017 4:39 PM

Deleted: e-f

Naveen Negi 7/31/2017 4:39 PM

Deleted: -d



751  
752  
753  
754  
755  
756

Figure 2: (a) The map of the regional divisions (shaded) for the time series analysis. (b-l) Time series of XCH<sub>4</sub> over the selected regions (shown in map) as obtained from GOSAT and simulated by ACTM for two different emission scenarios, namely, ACTM\_AGS and ACTM\_CTL. The gaps are due to the missing observational data.

Naveen Negi 7/31/2017 4:43 PM

Deleted:

Unknown  
Formatted: Font:(Default) Times New Roman, 10 pt

Naveen Negi 7/31/2017 4:39 PM

Deleted:

Legend: ● GOSAT

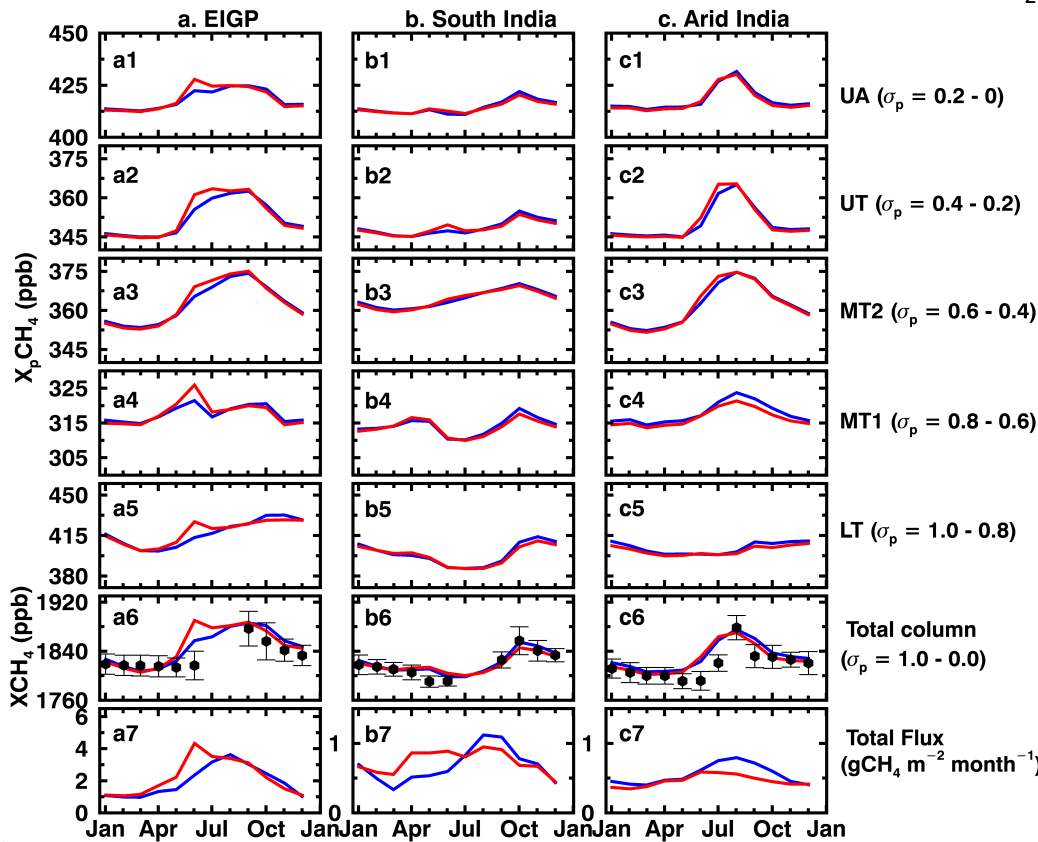
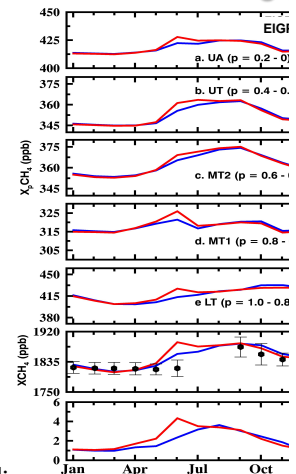


Figure 3: The bottom panels show the monthly mean climatology of the total optimized  $\text{CH}_4$  emissions (panels a7, b7, c7); estimated after performing the global inverse analysis (Patra et al., 2016). The second bottom panels show  $X\text{CH}_4$  obtained from the GOSAT observations (black circles in panels a6, b6, c6) and ACTM simulations (panels a6, b6, c6) over the Eastern IGP (a: first column), Southern Peninsula (b: second column) and Arid India region (c: third column). Monthly climatology is based on the monthly mean values for the period of 2011-2014 for all the values. The error bars in the GOSAT monthly mean values depict the 1-sigma standard deviations for the corresponding months (a6, b6, c6). The 1-sigma values are not plotted for the model simulations to maintain figure clarity. Simulations are based on two different emission scenarios namely ACTM\_CTL (blue lines) and ACTM\_AGS (red lines) based on the different combinations of emissions. The upper five panels show the monthly climatology of partial columnar methane (denoted by  $X_p\text{CH}_4$ ) calculated at five different partial sigma-pressure layers: 1.0-0.8 (a5, b5, c5), 0.8-0.6 (a4, b4, c4), 0.6-0.4 (a3, b3, c3), 0.4-0.2 (a2, b2, c2) and 0.2-0.0 (a1, b1, c1). Please note that the y scales in the emission plots over southern peninsula and Arid India (b7 and c7) are different from over the EIGP region (a7).

Unknown

Formatted: Font:(Default) Times New Roman, 10 pt, Bold

Naveen Negi 7/31/2017 4:50 PM



Deleted:

Naveen Negi 7/25/2017 12:07 PM

Deleted: ...f the total optimized  $\text{CH}_4$  ... [93]

Naveen Negi 7/31/2017 4:40 PM

Deleted: Figure 3: The bottom panels show the monthly mean climatology of the total optimized  $\text{CH}_4$  emissions (panels g, n, u); estimated after performing the global inverse analysis (Patra et al., 2016). The second bottom panels show  $X\text{CH}_4$  obtained from the GOSAT observations (black circles in panels f, m, t) and ACTM simulations (panels f, m, t) over the Eastern IGP (first column), Southern Peninsula (second column) and Arid India region (third column). Monthly climatology is based on the monthly mean values for the period of 2011-2014 for all the values. The error bars in the GOSAT monthly mean values depict the 1-sigma standard deviations for the corresponding months (f, m, t). The 1-sigma values are not plotted for the model simulations to maintain figure clarity. Simulations are based on two different emission scenarios namely ACTM\_CTL (blue lines) and ACTM\_AGS (red lines) based on the different combinations of emissions. The upper five panels show the monthly climatology of partial columnar methane (denoted by  $X_p\text{CH}_4$ ) calculated at five different partial sigma-pressure layers: 1.0-0.8 (e, l, s), 0.8-0.6 (d, k, r), 0.6-0.4 (c, j, q), 0.4-0.2 (b, l, p) and 0.2-0.0 (a, h, n). Please note that the y scales in the emission plots over southern peninsula and Arid India (n and u) are different than over the EIGP region (g).

761

762

763

764

765

766

767

768

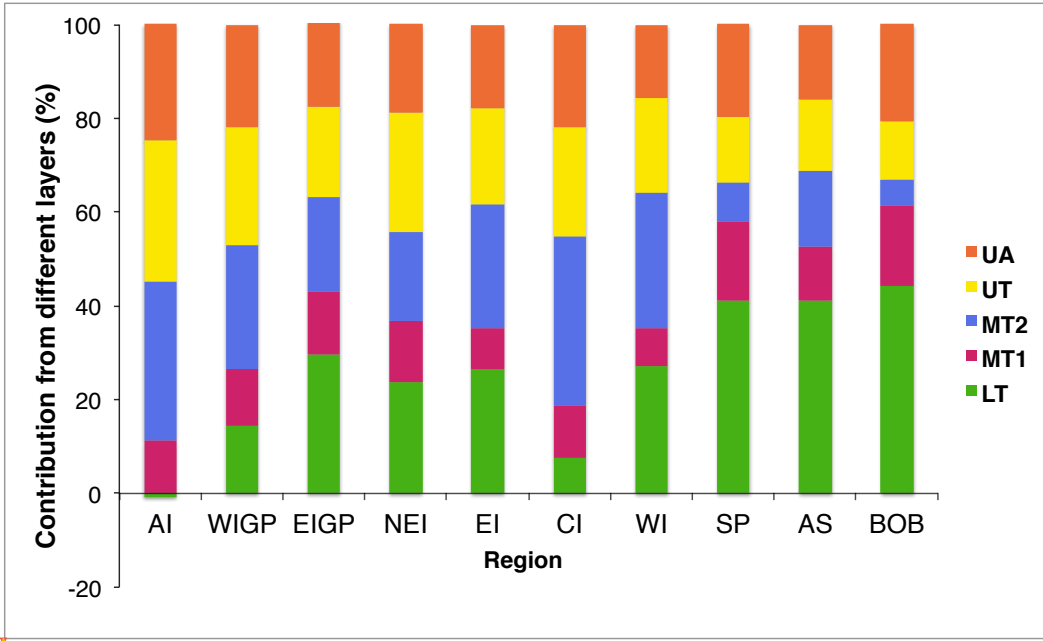
769

770

771

772

773



858

859 Figure 4: Contributions of partial columns in the seasonal amplitude of XCH<sub>4</sub> over selected regions for AGS case. Differences in  
 860 the X<sub>p</sub>CH<sub>4</sub>, calculated at the same time as the maxima and minima of the seasonal XCH<sub>4</sub> cycle, are used to calculate the  
 861 percentage contributions of respective partial columns in the seasonal amplitude of XCH<sub>4</sub>.

Naveen Negi 7/31/2017 4:50 PM

Deleted: -20

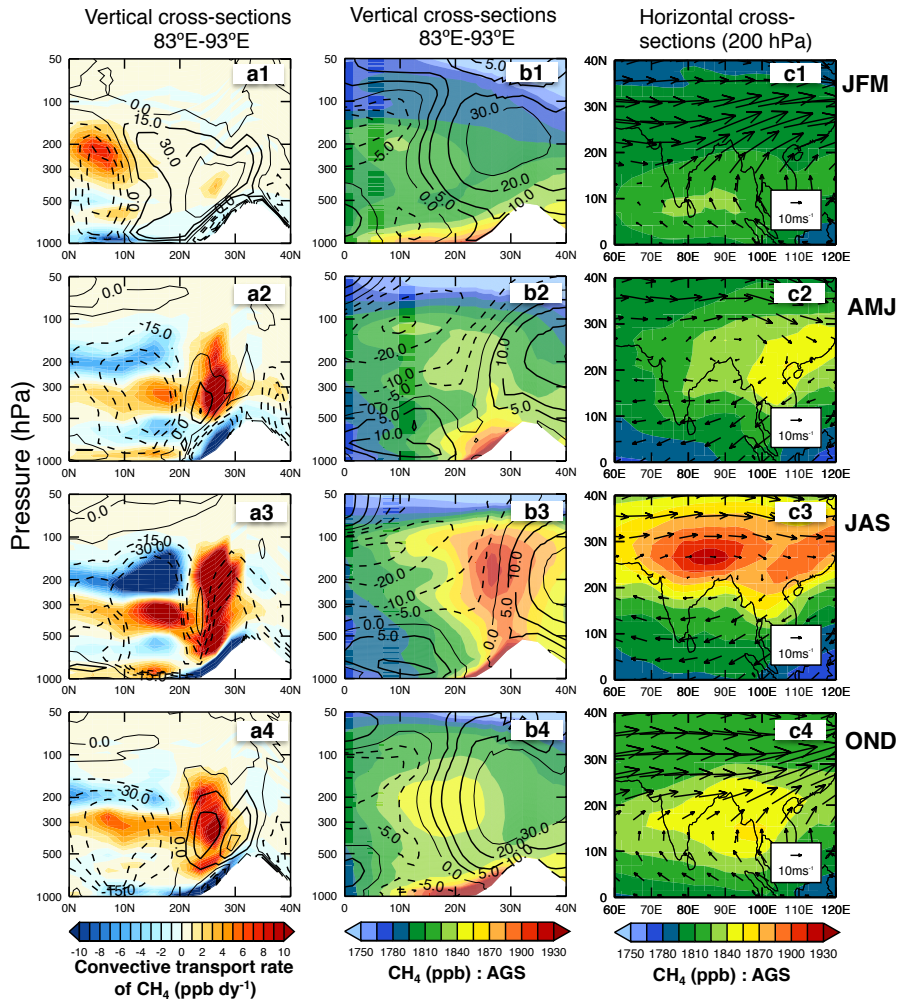
Unknown

Formatted: Font:(Default) Times New Roman, 10 pt

Naveen Negi 7/3/2017 12:26 PM

Deleted: cd





867

868

869

870

871

872

873

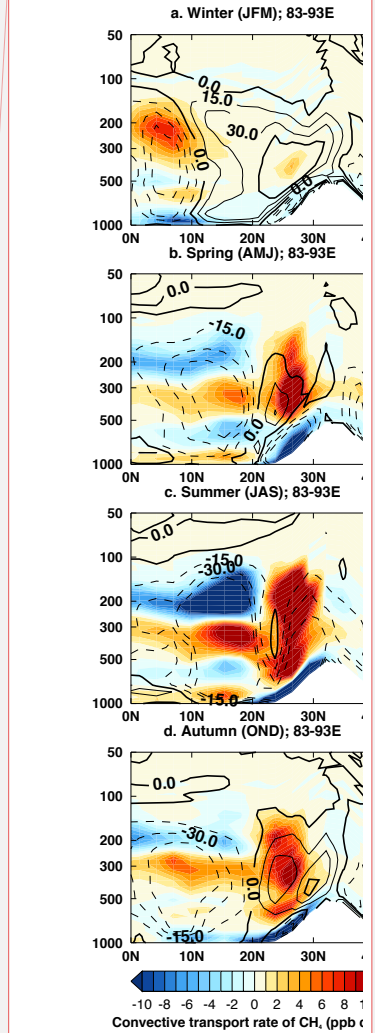
874

875

876

**Figure 5:** Vertical structure of seasonally averaged  $\text{CH}_4$  transport rate due to the convection (a1-a4, in  $\text{ppb day}^{-1}$ ) and  $\text{CH}_4$  mixing ratios (b1-b4 from AGS scenarios) averaged over 83-93 E for the year 2011. Positive and negative transport rate values represent the accumulation and dissipation of mass, respectively. The contour lines in the first (a1-a4) and second (b1-b4) columns depict the average omega velocity (in  $\text{hPa s}^{-1}$ ) and u wind component, respectively for the same period. The solid contour lines show the positive values and dotted lines show negative values. Positive and negative values of the omega velocity represent downward and upward motions, respectively. The zero value of u wind indicates that the wind is either purely southerly or northerly. White spaces in zonal-mean plots (a1- b4) show the missing data due to orography. The rightmost column (c1-c4) depicts the maps of averaged  $\text{CH}_4$  and wind vectors (in  $\text{m s}^{-1}$ ; arrow) during all the four seasons in 2011 at 200 hPa height.

Naveen Negi 7/31/2017 4:51 PM



Deleted:

Unknown

Formatted: Font:(Default) Times New Roman, 10 pt

Naveen Negi 7/20/2017 3:33 PM

Deleted: d... in  $\text{ppb day}^{-1}$ ) and  $\text{CH}_4$  mi... [94]

Naveen Negi 8/14/2017 2:48 PM

Formatted: Tabs:Not at 1.81"